

GRINDING STUDIES ON ATOMIZED BRASS PARTICLE

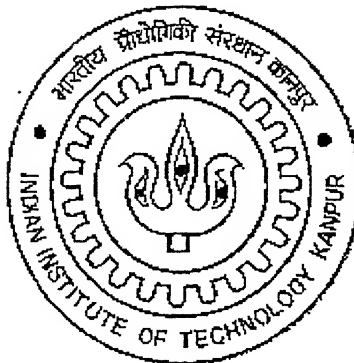
A thesis Submitted

In partial fulfillment of the Requirement for the Degree of

Master of Technology

by

SUSHANT KUMAR BADJENA



to the

DEPARTMENT OF MATERIALS AND METALLURGICAL ENGINEERING

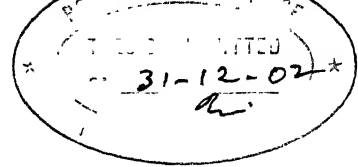
INDIAN INSTITUTE OF TECHNOLOGY, KANPUR

December 2002

पुस्तकोत्तम काशीनगर प्रस्तकालय
पार्वतीमुख कृष्णनगर
बाबापिता क्र० A 143503



A143503



CERTIFICATE

It is certified that the work contained in this thesis title “*Grinding studies on atomized brass particle*”, by Sushant Kumar BadJena, has been carried out under my supervision and that this work has not been submitted elsewhere for a degree.

Date: 31.12.2002

Dr. B.K. Mishra

Professor

Department of Materials and

Metallurgical Engineering

I.I.T Kanpur

Acknowledgments

I would like to express my deep gratitude to Dr. B.K. Mishra for their expert guidance, support and encouragement though out my graduate studies at Kanpur.Their leadership was immeasurable help to my early identification of an industrially significant area of research.

I would also like to acknowledge greatly to Dr. S. Bhargav for his immense help for making this work successful.

I would like to convey my sincere thanks to Mr. Suren Agnihotri, Mr K.S. Tripathy and Mr. Abinash Sahani for sincere help during the course of experimental work.I would like to thank Sanjeev bhai, Kamala, Gyanda, and Vishal Verma for all their help while writing the thesis.

I must acknowledge the support provided by my entire family and someone special for me. I would not have come this far without their unconditional love and support. This thesis is dedicated to them.

Finally I would like to mention those integral part of my IITK life, my friends, who have made every moment of stay here at IITK to rejoice in future.

ABSTRACT

Flaky metal powders commonly used as paint and pigments, are generally produced by grinding in ball mills or vibration mills. The key to good quality powder production is to optimize the processing parameters. In the present work grinding of brass particles is studied in detail in a laboratory size ball mill to determine the optimal levels of ball to material ratio, type and amount of additives, mill speed, ball load, etc. The quality of the powder is assessed on the basis of water coverage, degree of flattening and luster by visual inspection. Preliminary results in a 35-cm diameter ball mill with 30% ball load show that a material to ball ratio of 0.067 and a 0.1% dosage of stearic acid is what is required for good quality powder production.

For determining optimal mill speed and ball size a 2^2 factorial design work has been carried out. It has been determined that for best powder quality the mill must run at 70% critical speed and the ball size must not exceed 20 mm. The quality of the powder assed through scanning electron microscope and laser particle size analyzer compares very well with the industrial samples.

As a case study plant data collected from the industry is analyzed and processes to prescribe optimal processing parameters. Using Millsoft[®] it is established that the performance of the industrial mill can be improved by decreasing the speed, increasing the ball load and increasing the number of lifters. This is expected to increase the capacity of the mill while drawing maximum power and producing good quality powder.

CONTENTS

ABSTRACT	II
List of Tables	V
List of Figures	VII
1. Introduction	1
1.0 Technical Background	1
1.1 Melting practice	2
1.2 Powder Production	3
1.2.1 Atomization	3
1.3 Annealing	6
1.4 Milling or grinding	6
1.4.1 Breakage Mechanism	8
1.4.2 Critical Speed	9
1.4.3 Additives	9
1.5 Polishing	11
1.6 Problem Identification	13
1.7 Thesis Objective	14

CONTENTS

ABSTRACT	II
List of Tables	V
List of Figures	VII
1. Introduction	1
1.0 Technical Background	1
1.1 Melting practice	2
1.2 Powder Production	3
1.2.1 Atomization	3
1.3 Annealing	6
1.4 Milling or grinding	6
1.4.1 Breakage Mechanism	8
1.4.2 Critical Speed	9
1.4.3 Additives	9
1.5 Polishing	11
1.6 Problem Identification	13
1.7 Thesis Objective	14

2. Grinding Studies	15
2.1 Experimental procedure	15
2.2 Selection of grinding parameters	16
2.2.1 Effect of ball to particle ratio	17
2.2.2 Effect of type and amount of additive	21
2.3 2^2 Factorial Design	25
2.3.1 Surface Response	28
2.3.2 Effect of mill speed and ball size	30
2.3.3 Water Coverage	33
2.4 Particle Characterization	34
2.4.1 Scanning Electron Microscopy	34
2.4.2 Size Distribution	39
3. Analysis of Industrial Data Using Millsoft	42
4. Conclusions	54
APPENDIX A	57
REFERENCES	66

List of Tables

2.1	Variation in water coverage and enlargement ratio with Ball-to-material ratio	19
2.2	Variation in water coverage and enlargement ratio with Different additives used	23
2.3	Variation of water coverage and enlargement ratio with Different percentage of stearic acid	25
2.4	Calculated response and percentage of error for degree of flattening	28
2.5	Calculated response and percentage of error for water coverage	28
3.1	Typical plant practice data	43
A.1	Cumulative undersize finer after 16hrs grinding, material to ball ratio=0.1	57
A.2	Cumulative undersize finer after 16hrs grinding, material to ball ratio=0.075	58
A.3	Cumulative undersize finer after 16hrs grinding, material to ball ratio=0.06	58
A.4	Cumulative undersize finer after 16 hrs of grinding with stearic acid	59
A.5	Cumulative undersize finer after 16hrs grinding with paraffin wax	59
A.6	Cumulative undersize finer after 16hrs grinding with oxalic acid	60
A.7	Cumulative undersize finer after 16hrs grinding with 0.4% stearic acid	60
A.8	Cumulative undersize finer after 16hrs grinding with 0.3% stearic acid	61
A.9	Cumulative undersize finer after 16hrs grinding with 0.2% stearic acid	61
A.10	Cumulative undersize finer after 16hrs grinding with 0.1% stearic acid	62
A.11	Cumulative undersize finer after 16hrs grinding with 80% c.s and existing ball.	63
A.12	Cumulative undersize finer after 16hrs grinding with 60% c.s and existing ball	63

A.13 Cumulative undersize finer after 16 hours grinding with 80% c.s and 12mm ball (dia)	64
A.14 Cumulative undersize finer after 16hrs grinding with 60% c.s and 12 mm ball (dia)	64
A.15 Cumulative undersize finer after 16hrs grinding with 70% c.s and mix ball (first 8hrs with existing ball and next 8hrs with 12 mm ball)	65

List of figures

1.1	Typical flow sheet for producing metal powder in an industrial process.	2
1.2	Typical open circuit grinding for producing brass metal powders.	7
1.3	Typical close circuit grinding for producing brass metal powders.	7
1.4	Schematic and mathematical representation of (a) particles and fines,(b) flattening mechanism, (c) attrition mechanism and (d) breakage mechanism.	8
1.5	Chemical structure of stearic acid.	10
2.1	Water coverage measuring container.	16
2.2	Variation in weight mean diameter with time – effect of material to ball ratio (Mill speed = 70% critical; mill filling = 30%).	18
2.3	Particle size distribution after 16 hours of grinding - effect of material to ball ratio (mill speed = 70% critical; mill filling = 30%).	20
2.4	Disappearance plot - effect of material to ball ratio (mill speed = 70% critical; mill filling = 30%).	20
2.5	Variation in weight mean diameter with time – effect of additive type (mill speed = 70% critical; mill filling = 30%).	22
2.6	Particle size distribution after 16 hours of grinding – effect of additive (mill speed = 70% critical; mill filling = 30%).	22
2.7	Variation in weight mean diameter with time – effect of amount of additive addition (mill speed = 70% critical; mill filling = 30%).	24
2.8	Particle size distribution after 16 hours of grinding – effect of percentage of additive (mill speed = 70% critical; mill filling = 30%).	24

2.9 Two-level factorial designs for the factors Percentage of critical speed and ball size.	27
2.10 Surface plots for two measured responses: top— degree of flattening; below— water coverage	29
2.11 Variation in weight mean diameter with time; Experimental conditions at A, B, C, D, and E are defined in Fig. 2.10	31
2.12 Size distribution after 16 hours of grinding; Experimental conditions at A, B, C, D, and E are defined in Fig. 2.10.	31
2.13 Variation in the water coverage with the amount of fines (-45 micron)	33
2.14 Typical SEM images of the Orion powder sample (a) aggregate at 500X (b) Single particle at 5000X	35
2.15 Typical SEM images of the Mepco powder sample (a) aggregate at 500X (b) single particle at 5000X	36
2.16 Typical SEM images of the English powder sample (a) aggregate at 500X (b) Single particle at 5000X.	37
2.17 Typical SEM images of the Stearic acid powder sample (a) aggregate at 500X (b) Single particle at 5000X	38
2.18 Particle size distribution of as received powder sample obtained from the three different sources: Orion, Mepco and English.	40
2.19 Particle size distribution of powder sample after 16 hours of grinding.	41
3.1 Charge motion inside the tumbling mill (first stage grinding) at 42 rpm.	44
3.2 Lifter profiles used in the simulations (All dimensions are in mm).	45

3.3	Snapshots of charge motion inside the mill (Mill diameter = 0.8 m; ball load = 10%; ball diameter = 12 mm; mill speed = 26 rpm; power draft = 7KW).	47
3.4	Snapshots of charge motion inside the mill (Mill diameter = 0.8 m; ball load = 10%; ball diameter = 12 mm; mill speed = 32 rpm; power draft = 9KW).	48
3.5	Snapshots of charge motion inside the mill: effect of lifter configuration (mill diameter = 0.8 m; ball load = 20%; ball diameter = 12 mm; mill speed = 26 rpm).	50
3.6.	Snapshots of charge motion inside the mill: effect of lifter shape; (mill diameter = 0.8m; ball load = 20%; ball diameter = 12 mm; mill speed: (a) 26 rpm (b) 30 rpm (c) 36 rpm).	51
3.7	Impact energy spectra for two different mill simulations where only the ball size was changed.	52

CHAPTER-1

INTRODUCTION

Metals in the form of fine powders are used in a number of industries like powder metallurgy, paint and pigments, space, electronic, defense, etc. Metal powders can be produced by different methods such as atomization, precipitation, communution etc. Communution by ball milling is the most commonly used method for the production of flaky metal powders.

Flaky metal powders are generally produced by grinding in ball mills or vibration mills [1-4]. The characteristic feature that are unique to the mill product, namely luster and flakiness, are highly desirable properties of paints pigments for shining and better coverage capacity of the paints. In spite of the technological importance of this method there exists no fundamental process engineering analysis of grinding of metal powders. Sureshen *et al.* [5, 6] have reviewed the work in this area and carried out a detailed experimental study of vibration milling of aluminum powder.

The mechanisms of size reduction of metal powders are found to be somewhat different from that of brittle solids because of the ductile nature of the particles. A detailed study using scanning electron micrographs of the powder revealed that a combination of flattening, attrition and breakage are responsible for the size reduction of ductile metal powders [7]. Brittle materials, on the other hand, break by attrition, shatter, and cleavage. It is the predominant mechanism of breakage in either material that has drawn most attention both from a theoretical as well as practical point of view.

1.0 Technical Background

Ultrafine metal powders, such as brass and bronze for decorative paints and inks are prepared in several stages. The processing steps include melting, atomization,

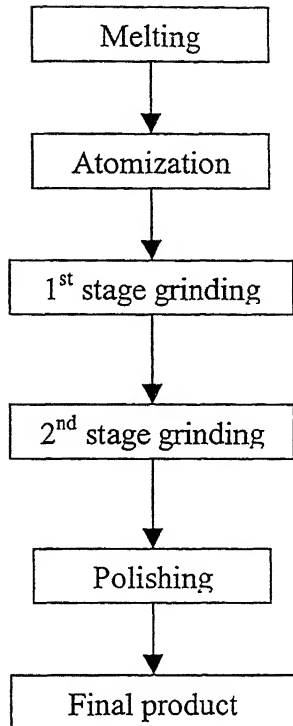


Figure 1.1 Typical flow sheet for producing metal powder in an industrial process.

annealing, grinding and polishing. The sequence of operation is shown in Fig. 1. Of all the processing steps, atomization and grinding are the two most important steps. Although the literature is filled with references to the atomization technique, there are very few references available on the processing of metallic powders by grinding. It is in this context that the research work described in this thesis assumes importance

1.1 Melting practice

The first step in metal powder production is to obtain the right kind of alloy or melt. This is typically done in a furnace where the solid metal is heated to a molten state. Alloying additions are made to obtain the required composition. The molten metal is then poured into a tundish that is used for atomization purpose. The main emphasis in the melting practice is to minimize contamination of any kind. For example, Atomization refers to the process of breaking of liquid into fine droplets. Thus any material in the molten state can be atomized. The terms nodulization and atomization are both synonymous and the former word is sometimes used for gas atomization in the chemical

industry. The product, a suspension of very fine liquid droplets can be described as an aerosol. Breakup of the liquid into discrete particles can be brought about by impingement with water or gas, often termed two-fluid atomization. Alternatively centrifugal force may be used to break-up the liquid stream. Atomization also occurs if the liquid metal containing a gas under positive pressure is exposed to vacuum

1.2 Powder Production

Essentially all the materials can be made into powder form. But the selection of particular fabrication method depends on the properties of the material and process economics. There is always a correlation between the powder fabrication mode, size and shape microstructure and chemistry of the powder product. There are a seemingly unlimited number of powder fabrication modes. Metal powders are produced commercially by one of four approaches: chemical, electrolytic, mechanical and atomization. The diversity in size, shape and surface morphology of powders reflects the underlying conditions that control the formation of the metal or alloy in a finely divided form. The size, shape and external and interior structure of the atomized powders has been discussed here as it is relevant to the present thesis.

1.2.1 Atomization

Atomization is defined as the process of breaking of liquid into fine droplets. Thus any materials in the molten state can be atomized. The terms Nodulization and atomization are both synonymous and the former word is sometimes used for gas atomization in the chemistry industry. The product, a suspension of very fine liquid droplets or solid particles in a gas, can be described as an aerosol. Breakup of the liquid into discrete particles can be brought about by impingement with water or gas, often termed two-fluid atomization. Alternatively centrifugal force may be used to breakup the liquid stream. Also if the liquid metal containing a gas under positive pressure is exposed to vacuum, atomization occurs.

There are several interrelated and compelling reasons that high powder production rates give economy of scale: in the production of iron powders by water atomization with metal feed rate up to about 400 kg/min [8]. In several mode of atomization, control of the size, shape and surface morphology of the powder particles is possible. Similarly, with atomization, a high degree of alloying flexibility exists, accompanied by control of impurity labels. Each atomized particles is a pre alloy or mini-ingot and the composition is essentially identical from particle to particle. Apart from iron powder production, high quality powders of aluminum, copper, stainless and a wide range of ferrous and non-ferrous especially alloy powders are now manufactured by atomization.

Gas atomization

Non-ferrous metal powders have been produced since the 1920's by air atomization. This early technology was based primarily on the use of a single spray nozzle for disintegration of the molten metal [9, 10, and 11]. Initially the two-fluid gas atomization was simulated by a chemical processing industry [12] in their need to atomize a wide range of liquids with diverged properties (e.g. oils, chemical solutions, emulsions and dispersions, slurries and gels). Adaptation of two-fluid atomization methods for the production of steel powders dates back to world war-II, when the Mannes-mann process was developed in Germany for making iron powder by air atomization. Over the last four decades, two-fluid gas atomization technology has matured and powders of aluminum, copper, iron, low alloy steels, super alloys, tin, and tool steels are now made on a tonnage scale for a range of application over the last decade.

The worldwide annual tonnage of inert gas atomized metal powders is much less than that for water atomized powders. Air atomization of aluminum, brass, copper and zinc powders accounts per about 250, 00 metric tons per year. Inert gases are used when the oxygen content is low, or when the metals are reactive such as super alloys and titanium. Metal feed rates are lower than in water atomization and the highest rate achieved is 120kg/min [13]. The world capacity for producing inert gas atomized

powders is estimated to be at least 40,000 metric tons per year, but this is under utilization in the present day scenario.

Gummerson *et al* [14] have given general descriptions for gas atomization. There are similarities in the design of gas and water atomizer, particularly with respect to nozzle design. Nozzle takes the form of discrete openings or annular rings concentric with the metal stream .In addition a confined configuration is frequently used in gas atomization. This design is used almost exclusively with an annular nozzle and atomization occurs at the orifice of the nozzle and at the base of the tundish. The closed configuration is preferred in gas atomization for efficiency because of the rapid decay in velocity of the gas stream with distance from the nozzle.

The general features of a commercial gas atomization unit are similar to those of water atomization facility. Like water atomization, gas atomization involves many process variables with minor changes. Normally, the gas used to purge the atmosphere in the tank will be the same as the gas used for atomization. To minimize powder contamination all the internal surfaces of the chamber are fabricated from polished stainless steel.

Melting equipment and procedures described for water atomization are applicable to gas atomization. For reactive melts, induction melting is performed in vacuum. The flow rate of molten metal to the atomizing nozzle is generally smaller than in water atomization with low melting point metals, gas atomization is frequently performed on a continuous basis at rates between 8 and 33 kg/min [15].

Air and nitrogen are commonly used to disintegrate the stream of molten metal in gas atomization. To minimize contamination of reactive molten alloys, argon is most commonly used. Alternatively, helium provides an inert environment and also increases the cooling rate of the atomized droplets. Mixtures of gases can be selected to achieve desire powder characteristics at lowest cost. Dopants in the gas are now generally being used for passivity of the surfaces of active powders.

Gas atomized powders are typically spherical in shape with smooth surfaces. Small satellite particles are frequently seen attached to larger particles. Mass median of particle size is normally in the range 50 to 300 μm with a standard deviation of about one order of magnitude, which is lower than that in water atomization. Aluminum based materials, zinc and copper-zinc alloys are an exception since the irregular particle morphology of air atomized powders resembled that of a water-atomized powder.

1.3 Annealing

Annealing has different meaning in the context of metal powder production as opposed heat treatment processes. Here annealing refers to the removal of oxides from the surface of atomized particles. It is typically practiced in a furnace in a controlled environment where the temperature and residence time of particles are maintained. Typically NH_3 is used for the removal of oxides species by allowing it to react with the ammonia gas at a suitable reaction temperature.

1.4 Milling or grinding

Grinding follows atomization in the process of metal powder production. Here the particles are reduced in size by a combination of impact and abrasion. It is performed in a rotating cylindrical steel vessel known as tumbling mills. These contain a charge of atomized metal particles and steel balls as the grinding medium, which is free to move inside the mill, thus comminuting the metal particles. In grinding close control of product size is important. For this reason, correct grinding is often said to be the key to good powder processing. It is important to realize of all stages of powder processing starting with melting up to polishing, grinding is the most energy intensive operation.

Structurally, tumbling mills consist of a horizontal cylindrical shell, provided with renewable wearing liners and a charge of grinding medium. The drum is supported so as to rotate on its axis on hollow trunnions attached to the end walls. The diameter of the mill determines the pressure that can be exerted by the medium on the particles and, in general the larger the feed size larger is the required mill diameter. The length of the mill,

in conjunction with the diameter, determines the volume, and hence the capacity of the mill.

The feed material is usually fed to the mill continuously through one end. The ground products leave via the other end or through a number of ports spaced around the periphery of the shell depending upon the application. All types of mill can be used for wet or dry grinding through modification of feed and discharge equipment.

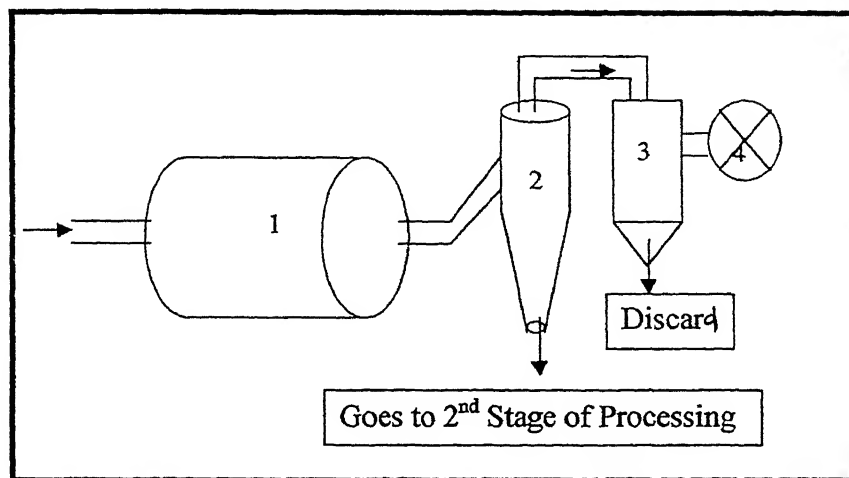


Figure 1.2 Typical open circuit grinding for producing brass metal powders.

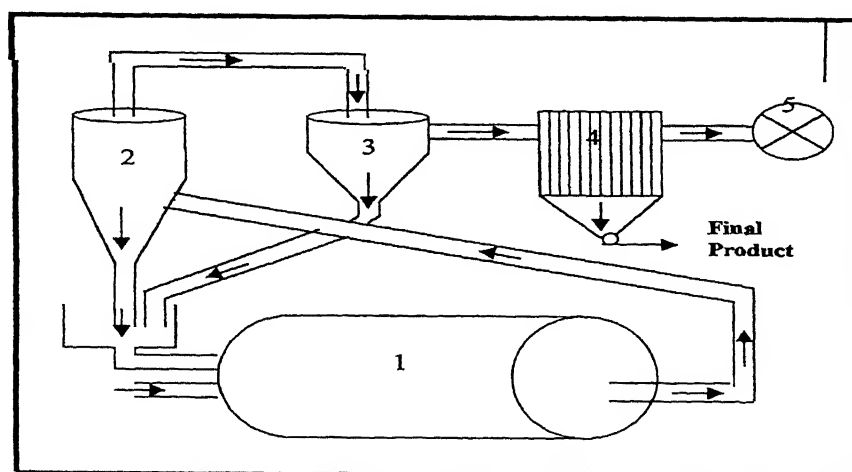


Figure 1.3 Typical close circuit grinding for producing brass metal powders.

Grinding can be practiced in open circuit or close circuit with help of a classifier. Schematics of both types of grinding are shown in Fig. 1.2 and 1.3. Closed circuit grinding with high circulating loads produces a closely sized end product and a high output per unit volume compared with open circuit grinding.

1.4.1 Breakage Mechanism

The mechanism of size reduction of metal powders is found to be somewhat different from that of brittle solids because of the ductile nature of the particles. A detailed study using scanning electron micrographs of the powder revealed that a combination of flattening, attrition and breakage are responsible for the size reduction of ductile metal powders.

Based on experimental observations and qualitative understanding of the grinding of metal powders following state of mechanistic representation are introduced.

- The particles are characterized by two independent variables α and β projected area diameter and thickness respectably.
- The grinding of metal powders proceeds through a combination of the mechanisms of flattening, attrition and breakage. A schematic representation, as well as the necessarily physical constrains associated with these three mechanisms, is included in Fig 1.4.

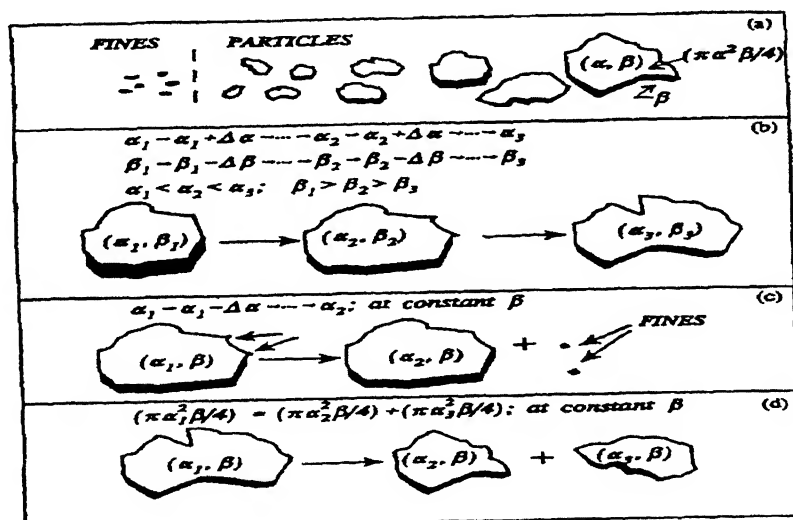


Figure 1.4: Schematic and mathematical representation of (a) particles and fines, (b) flattening mechanism, (c) attrition mechanism and (d) breakage mechanism.

In case of brass metal powder grinding flattening mechanism is predominant. As the grinding progresses metal powders became flat i.e. projected area diameter increases and thickness decreases. From the figure case (b) is predominant in case of our brass metal powder grinding.

There are several factors that affect the performance of tumbling mills. Among them critical speed is the important factor. Critical speed is calculated with the formula given below.

1.4.2 Critical Speed

$$n_c = \frac{1}{2\pi} \sqrt{\frac{g}{R - r}}$$

Where n_c = critical speed

R = ball mill radius

r = ball radius

1.4.3 Additives

The process of metal powder grinding includes mixing the particles with a suitable additive. During grinding, because of the large attractive forces between small particles the powder can be agglomerated. In order to avoid particle agglomeration in the powder, surface-active additives are used for enhancing the dispersion of the particles. To have a mixture free of agglomerates is important since agglomerates will affect the viscous behavior of the mixture. If the additive is to work properly as dispersant it must interact with the powder surface and ideally adsorb onto it. Thus, not only is the chemical character of the additive itself is important, but also the chemical properties of the powder surface. Metal powder has a surface layer of one or more oxides. Thus, the presence of oxides also impacts the way the powders interact with the additives during grinding.

Stearic Acid

Stearic acid is an example of a fatty acid. Fatty acids are long molecules consisting of a hydrocarbon chain with a carboxylic acid (-COOH) group. The long tail of the molecule, made up of carbon and hydrogen, is not attracted to water and is said to be hydrophobic (literally water fearing). The carboxylic acid “head” can form hydrogen bonds with water, and is therefore strongly attracted to water. It is said to be hydrophilic (literally water –loving). When a fatty acid is placed on water surface, the hydrophilic heads of the molecules are attracted to the water. As a result the molecules from a monolayer on the surface of the water with their heads sticking into the water and their hydrophobic tails sticking above the surface of the water.

Stearic acid, C₁₈H₃₆O₂

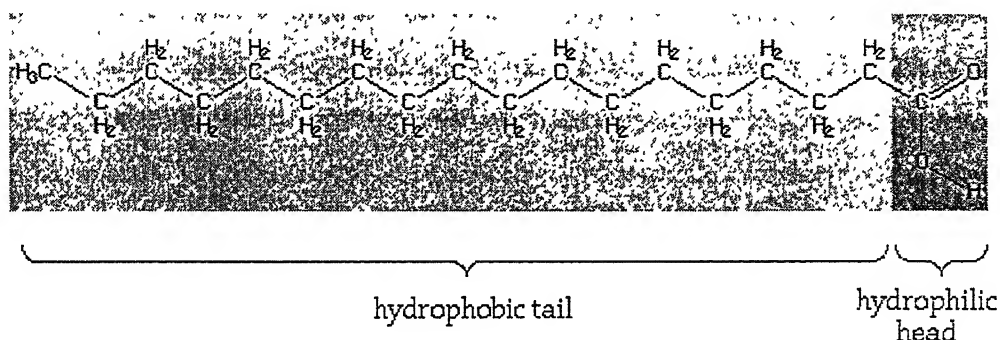


Figure 1.5 Chemical structure of stearic acid

Writing out all of these C's and H's in the diagram of the molecule can get tedious. They can also obscure the underlying structure of the molecule. Therefore, common shorthand is to leave them out. In the following diagram, at the points where line segments join, it is understood that a carbon atom is present with enough hydrogen's to make sure all of the carbon bonds are filled.

Paraffin Wax

The wax present in petroleum crudes primarily consists of paraffin hydrocarbons (C18 - C36) known as paraffin wax and naphthenic hydrocarbons (C30 - C60). Hydrocarbon components of wax can exist in various states of matter (gas, liquid or solid) depending on their temperature and pressure. When the wax freezes, it forms crystals. The crystals form of paraffin wax is known as microcrystalline wax. Those formed from naphtenes are known as microcrystalline wax .

Oxalic acid

Oxalic acid as $\text{HO}_2\text{CCO}_2\text{H}$, is a colorless, crystalline organic carboxylic acid that melts at 189°C with sublimation. Oxalic acid and oxalate salts are poisonous. Oxalic acid is found in many plants, e.g., sorrel and rhubarb, usually as its calcium or potassium salts. Oxalic acid is the only possible compound in which two carboxyl groups are joined directly. For this reason oxalic acid is the one of the strongest organic acids. Unlike other carboxylic acids (except formic acid), it is readily oxidized, which makes it useful as a reducing agent for photography, bleaching, and ink removal. Oxalic acid is usually prepared by heating sodium formate with sodium hydroxide to form sodium oxalate, which is converted to Calcium oxalate and treated with sulfuric acid to obtain free oxalic acid.

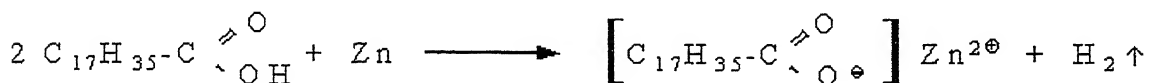
1.5 Polishing

After grinding the particles are polished in presence of grinding additives to impart luster. Thus decoloration is a major bottleneck in marketing of metal powder. Decoloration is a particle surface specific phenomenon. On the surface chemical changes due to decoloration could take place due to the following mechanisms:

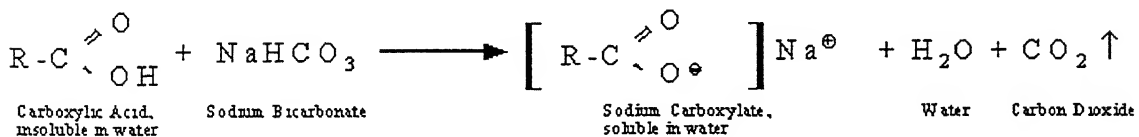
- Deterioration of the surface protective agents (long-term effect)
- Formation of a second phase compound on the surface (short-term effect)

products. In the UV curing process, ultra-violet light interacts with specially formulated chemistries to cure coatings that become UV resistant. UV curing is developed and marketed by CIBA especially for the printing, packaging, electronic and wood products industries. It is recognized as an “enhancement technology,” that allows manufacturers to make their products more attractive and durable. It also allows the printing and ink industries to achieve the highest gloss attainable by any coating method.

Formation of a second phase on the surface is based on the hypothesis that the stearic acid reacts with the zinc substrate to form a salt of the acid according to the following scheme:



The formation of carboxylates (salt), also designated as salification, is a well known method in organic chemistry for identification and isolation of carboxylic acids. Alkaline salts of carboxylic acids (e.g. Na, K) are soluble in water and insoluble in non-polar solvents. Heavy metal salts (e.g. Fe, Cu, and Zn) on the other hand are insoluble in water. That means for example, a non-identified organic compound which is insoluble in water but soluble in aqueous sodium bicarbonate, must be a carboxylic acid. It obviously forms the sodium salt first and this sodium carboxylate then is soluble in water:



Salification of carboxylic acids and the use in organic chemistry usually can be found in any handbook for organic chemistry.

1.6 Problem Identification

As far as the industrial grinding practice is concerned mill optimization is necessary for assurance of improved quality and productivity. But the problem of mill optimization is intimately related to the quality of the atomized powder, mill operational parameters, cyclone performance, etc. Therefore, the scope of the present research is restricted to problems concerning grinding/milling practice.

In order to get suitable combination of better coverage and best productivity, it is necessary to vary the key variables of a particular size reduction operation that typically involves several stages of grinding. The different milling or grinding parameters that affect the quality of powder are as follows:

- Amount of ball – to – powder ratio
- Type of additive
- Amount of additive – to – powder ratio
- Mill speed
- Mill filling
- Ball size and distribution
- Lifter shape and configuration

1.7 Thesis Objective

The present work involves a detailed laboratory investigation to determine the correct grinding parameters such as ball to particle ratio, type and amount of additives. Once these values were set an experimental design involving two key variables namely mill speed and ball size was formulated. The resulting optimal parameters were decided based on the water coverage and degree of flattening involved.

The objectives of the present work are as follows

1. To experimentally optimize the ball mill to get better shining and water coverage.
2. To find out the optimum material to ball ratio for effective use of impacts of balls inside the mill which in turn give rise to improved energy utilization.
3. To find out the best additives for the grinding operation of brass powder
4. To find out the percentage of additive used which will give better water coverage and shining property.
5. Optimization of mill speed and ball size through a 2^2 factorial design analyzing the combined effect of the effect of some key variables on the quality of powder.
6. Analysis of plant milling situation with the help of a software (Millsoft[®])[16], to identify plant bottlenecks

CHAPTER 2

GRINDING STUDIES

This chapter is concerned with the laboratory experimental work relating to grinding behavior of 70-30 atomized brass particles. Few preliminary tests were done to determine the correct grinding parameters such as ball to particle ratio, type of additives, and the amount of additives. Once these values were set an experimental design involving two key variables namely mill speed and ball size was formulated. The resulting optimal parameters were decided based on the water coverage and degree of flattening.

2.1 Experimental procedure

Atomized brass powders (70 wt % Cu and 30 wt % Zn), used in this investigation were supplied by M/s Orion Metal Powder Pvt. Ltd. Ranikhet, Uttaranchal, India. As received material were fed to the ball mill in different proportion depending on the type of tests conducted. The ball mill had an inner diameter and 35cm and a depth of 17.5 cm. There were altogether eight equally spaced square cross sectioned lifter bars mounted on the inside surface of the ball mill. In all the experiments the mill was filled up to 30 % of inner volume. Mill was placed over a rubber roller and rotated by a variable speed AC motor.

Experiments were conducted by adding different amounts of atomized particles and different types of additives with in varying proportions. In all the experiments additives were added at four hours of grinding intervals. After every four hours the mill was stopped and the material was carefully removed. These materials were then transfer into a sampling device called sample splitter that randomly divides the total sample into several fractions. One such fraction weighing approximately 300 grams was sieved to obtain the size distribution. Sieve sizes used for sieve analysis were in the range of 30 to 375 mesh or 600 to 45 μm . Sieving was done for 30 minutes in each experiment.

After the sieve analysis, a small amount of representative sample was kept for the measurement of water coverage, laser size analysis and optical and scanning electron microscopy wherever required.

Water coverage or leafing property measurement was carried out in a hollow container as shown in the Fig. 2.1. The container was always completely filled with water. A representative sample of 0.1 gram of powder was used for the analysis. The 0.1 gram sample was put in water and slowly mixed such that it nicely formed a film on water. The film was allowed to confine to an area bounded by the container wall and a moving slider. The area of the film was measured and the data reported as square centimeter per gram to represent the water coverage.

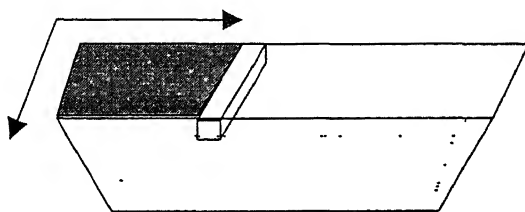


Figure 2.1 Water coverage measuring container

Size analysis by laser technique was carried out in a Fritch particle size analyzer. A representative ground sample was first dissolved in hexane to disperse the particles adequately. Then the sample was dried and sent for size analysis.

2.2 Selection of grinding parameters

Several experiments were carried out to find out the effect of various grinding parameters on the quality of the powder. These parameters are as follows:

- Ball/powder ratio
- Type of additive and dosage
- Mill speed
- Ball size
- Mill filling

The quality of the powder was assessed by considering the size distribution of the powder, particle enlargement ratio i.e. the average feed size of particles to that of the product size, water coverage, and visual assessment of the luster of the powder.

2.2.1 Effect of ball to particle ratio

The ratio of weight of balls to the particle inside the mill is a key factor that influences the grinding behavior of the particle. Too many particles tend to provide a cushioning effect that is detrimental for attaining optimal breakage rate of particles. On the other hand, too few particles lead to wastage of impact energy. Thus a compromise is sought between the grinding media mass and the amount of particles for a given size (size distribution of balls). Three grinding experiments were done using different amounts of atomized particles while keeping the ball weights same. Thus in these experiments the particulate material to ball ratio turned out to be 0.1, 0.075 and 0.06. Fig. 2.2 shows the variation in mass average particle size versus time. The average particle size of the particulate mass was calculated from the sieve analysis data. Initially, all the particles were in the size range of 300 to 500 micron. As grinding progressed, the average size increased due to flattening. The degree of flattening attained is dependent on the intensity of impact, initial size, and the composition of the particle.

During grinding the average size of particles invariably increases due to the intrinsic plastic behavior and then subsequently decreases due to breakage. Thus flattening of particles is expected during grinding. Assuming that for a mono-size particulate system the extent of flattening is similar for all particles, it is argued that the particles undergo two distinct modes of transformation leading to breakage. In the first stage the particle thickness decreases continually during grinding and in the second stage when the particles are sufficiently thinned breakage take place. Both stages of grinding can be analyzed by first order breakage kinetics.

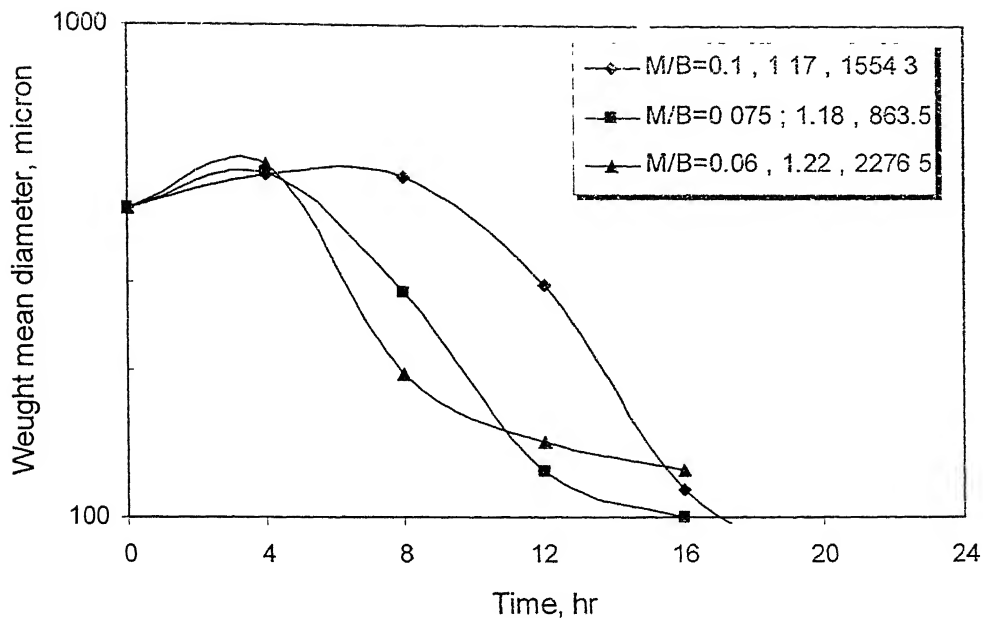


Figure 2.2 Variation in weight mean diameter with time – effect of material to ball ratio (Mill speed = 70% critical; mill filling = 30%).

The grinding data as shown in Fig. 2.2 and Fig. 2.3 reveal many interesting features pertaining to the breakage behavior of particles. Here the experimental result for three different materials to ball ratio (M/B) is presented. As mentioned earlier, flattening is evident since there is peak in all the curves. After certain time of grinding the average size begin to decrease indicating that the particles tend to break. In these experiments for M/B ratio of 0.06 and 0.075 particles tend to break around 4 hours of grinding. However, when M/B ratio was increased to 0.1 a prolonged flattening period was evident. This indicates a slower kinetics of the process for the first stage involving flattening. This is also evident from Fig. 2.3 that shows a bimodal distribution where presence of two groups of particles is evident. Although it is clear from the analysis of grinding data that a material to ball ratio of 0.06 is the best for faster breakage, the optimal parameter can be decided by considering several factors such as extent of flattening, rate of breakage, and the ultimate water coverage attained.

In Fig. 2.2, the legend shows two additional values. These represent the particle size enlargement ratio and the water coverage respectively. The water coverage and the

extent of flattening were highest for a material to ball ratio of 0.06. These data are presented in Table 2.1. Analyzing these data the optimal level of material to ball ratio was determined to be 0.06.

Table 2.1 Variation in water coverage and enlargement ratio with Ball-to-material ratio

Ball to material ratio	Water coverage (cm²/gm)	Degree of flattening
0.06	1130.5	1.22
0.075	580.9	1.18
0.1	502.4	1.17

Figure 2.4 shows the disappearance plot for the three different grinding conditions. Here a narrow size particulate sample between 30 and 60 mesh was used for grinding while varying the material ball ratio (mill speed = 70% critical, mill filling = 30%). The material remaining in this narrow size range was recorded while grinding was taking place at intervals of 4 hours. At the end the data is plotted as fraction of material remaining in the top size range versus time. Typically these sorts of data on log-linear scale yield a straight line suggesting first order breakage kinetics. However as evident from Fig. 2.4, the data do not conform to straight line suggested different breakage kinetics. Nevertheless, the relative position of the curve corresponding to M/B = 0.06 (material to ball ratio) suggest that the material in the top size range breaking at a faster rate compared to other two cases.

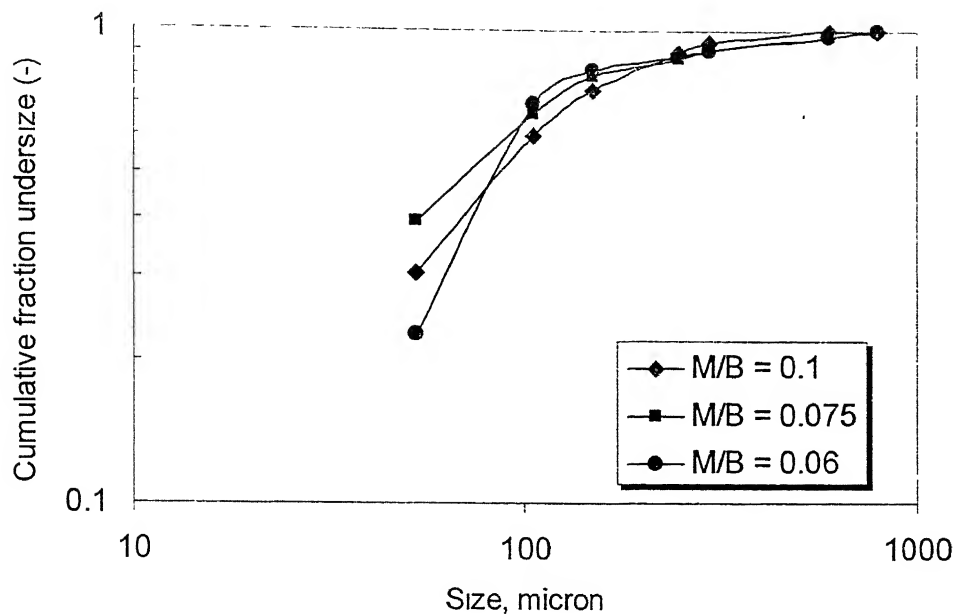


Figure 2.3 Particle size distribution after 16 hours of grinding - effect of material to ball ratio (mill speed = 70% critical; mill filling = 30%).

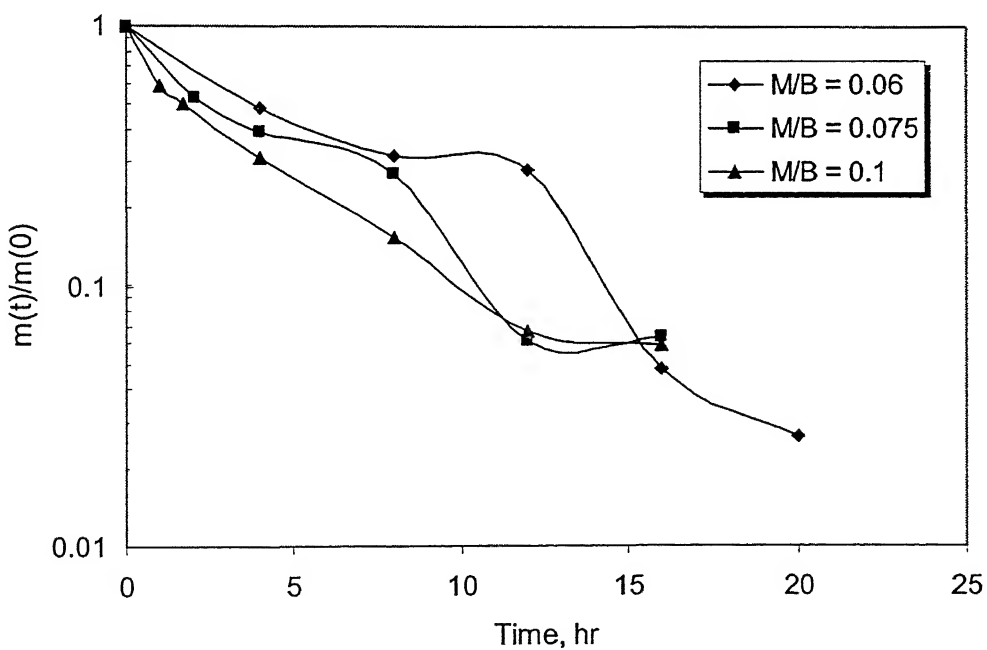


Figure 2.4 Disappearance plot - effect of material to ball ratio (mill speed = 70% critical; mill filling = 30%).

2.2.2 Effect of type and amount of additive

Grinding of metallic particles is typically carried out in presence of additives that help not only in plastic deformation but also in preserving the surface from undue oxidation and environmental attack. Since the additives are surface active agents, these are added in moderate quantities for monolayer coverage. Three types of additives are studied in these tests: stearic acid, oxalic acid, and paraffin wax. A brief description of these additives is already presented in chapter 1.

Several experiments were carried out by using three different types of additives: stearic acid, oxalic acid, and paraffin wax. Few tests were also done by using a combination of stearic acid and paraffin wax. A typical experimental result showing the grinding behavior is presented in Fig. 2.5. The three different curves represent the variation in the weight mean diameter with time for the three additives used. It is seen that stearic acid gives reasonably good flattening ratio and as seen from the legend of the figure, it also gives highest water coverage. The grinding data is presented in Fig. 2.6 that shows comparatively much finer distribution of powder after 16 hours of grinding with stearic acid. Considering the enlargement ratio and the water coverage coupled with the breakage data as presented in Fig. 2.6, it was very conclusively decided that the stearic acid has the best effect in terms maximizing both the water coverage and the enlargement ratio.

It should be pointed out that the paraffin wax served equally well as far as grinding is concerned. But excessive amount of blackening of the particles was observed during grinding. Since the luster of particles was one of the prime concerns, paraffin wax could not be used. Moreover, the water coverage of particles with paraffin wax turned out to be minimal.

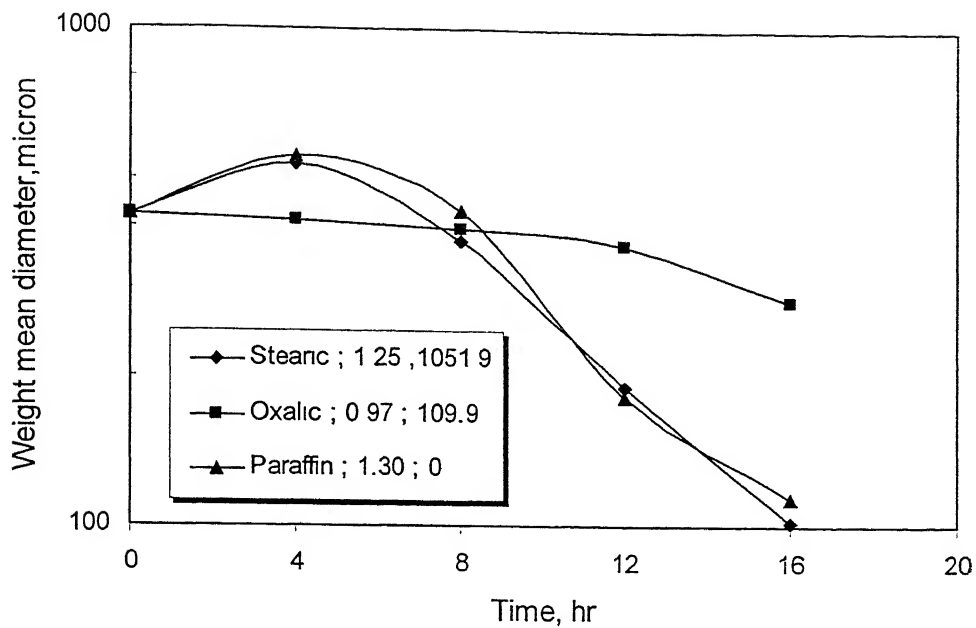


Figure 2.5 Variation in weight mean diameter with time – effect of additive type
(mill speed = 70% critical; mill filling = 30%).

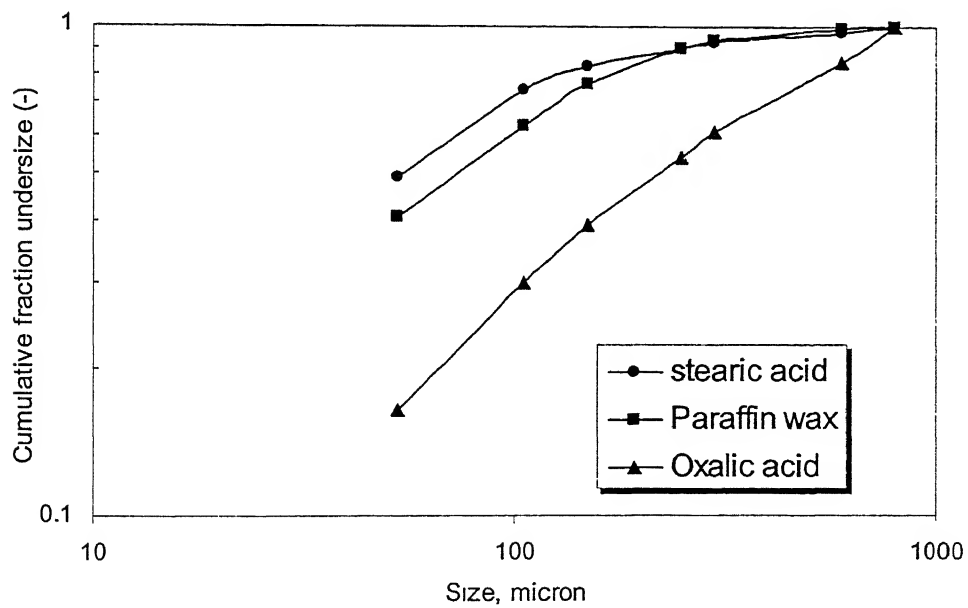


Figure 2.6 Particle size distribution after 16 hours of grinding – effect of additive
(mill speed = 70% critical; mill filling = 30%).

The amount of additives used in grinding plays a crucial role in influencing the ultimate powder properties. Thus optimal usage of the additive had to be determined. As mentioned earlier the additive to be used must serve not only to aid in the grinding

process but it must coat the particle surface without degrading the luster. To determine the optimal dosage several experiments were carried out using stearic acid. Stearic acid dosages were fixed at 0.1, 0.2, 0.3 and 0.4% of the total particle weight. The results of these tests are presented in Fig. 2.7. Although the water coverage increased with increase in stearic acid dosage, it has been found that there is a simultaneous decrease in the enlargement ratio beyond 0.2 % (of the material weight).

The grinding data is shown in Fig 2.8. This figure shows that after 16 hours of grinding the particle size distribution is more or less similar. Therefore, excessive amount of additive beyond a certain level do not help in grinding.

The water coverage was highest for particles ground with stearic acid, but degree of flattening was highest in case of paraffin wax. So combining these two factors i.e., degree of flattening and water coverage, the best additive was decided. The water coverage and flattening data are presented in Table 2.2. Analyzing these data stearic acid was determined to be the best additive. Like wise it was determined that 0.1 % percent of stearic acid addition is optimal with respect to water coverage and luster. These data are present in Table 2.3. One could use increase the stearic acid dosage from 0.1 % but it was determined that excessive amount stearic acid was detrimental to the luster of the particle.

Table 2.2 Variation in water coverage and enlargement ratio with Different additives used.

Additives used	Water Coverage (cm ² /gm)	Degree of Flattening
Stearic acid	1051.9	1.25
Oxalic acid	109.9	0.97
Paraffin wax	0	1.30

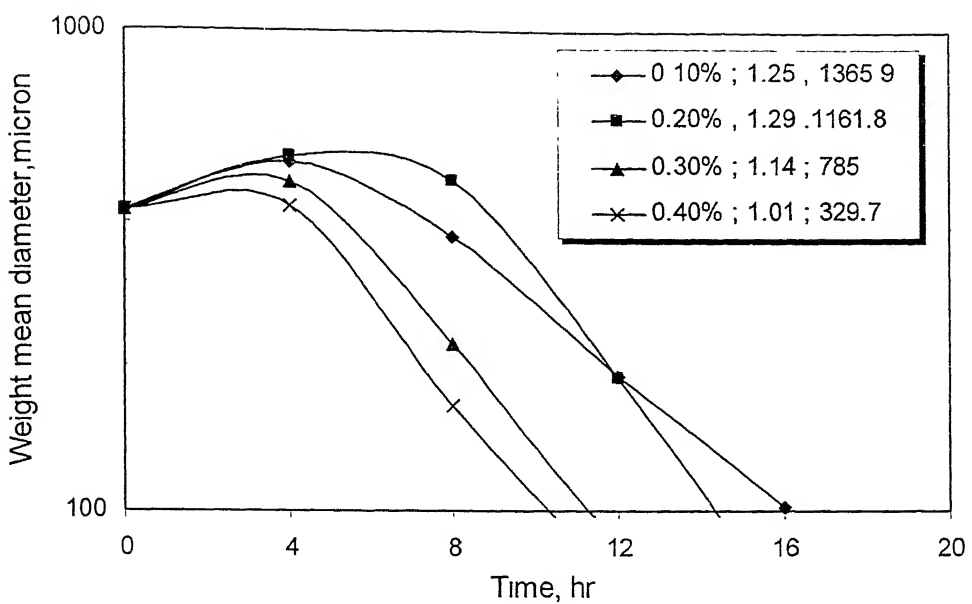


Figure 2.7 Variation in weight mean diameter with time – effect of amount of additive addition (mill speed = 70% critical; mill filling = 30%).

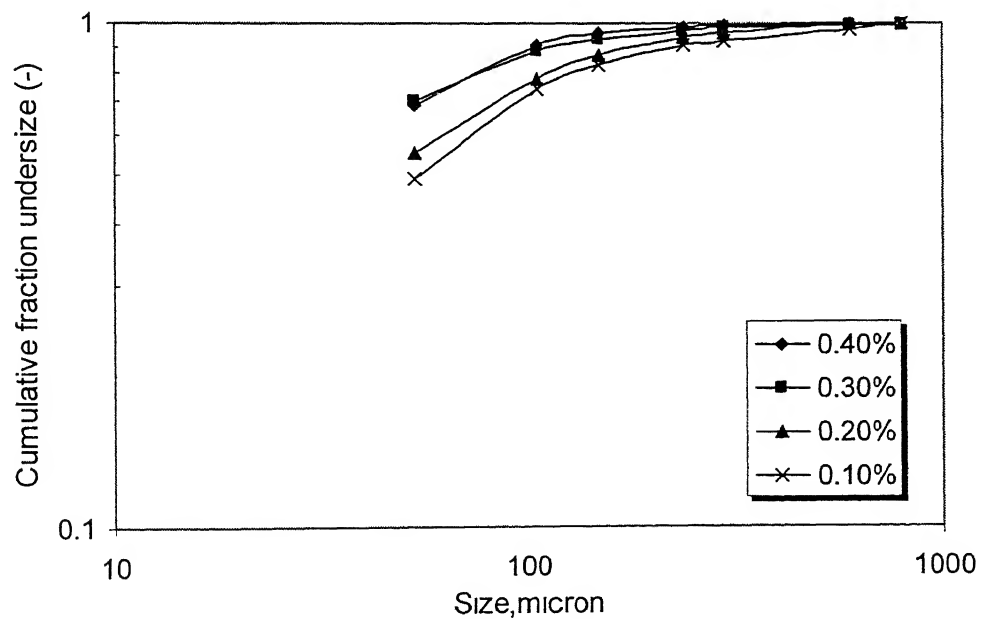


Figure 2.8 Particle size distribution after 16 hours of grinding – effect of percentage of additive (mill speed = 70% critical; mill filling = 30%).

Table 2.3 Variation of water coverage and enlargement ratio with Different percentage of stearic acid.

Percentage of Stearic acid	Water coverage (cm ² /gm)	Degree of Flattening
0.40	329.7	1.25
0.30	785	1.29
0.20	1161.8	1.14
0.10	1365.9	1.01

2.3 2² Factorial Design

Once the essential parameters such as particle to ball ratio, type and amount of additives and ball load (mill filling) were decided, the next step was to study the effect of mill speed and ball size. These parameters are important because unlike other parameters these typically cannot be changed during plant operation. Therefore, a two dimensional model was sought (2² Factorial Design) to study the effect of mill speed and ball size by considering one response at a time.

Here a model involving two geometric co-ordinates and one dependent variable is considered. By employing orthogonal design, the surface response method can be made most efficient. When the estimates of the coefficient are orthogonal, the sum of the squares of the deviations associated with the coefficients is also orthogonal, and thus maximum amount of information can be obtained for a given amount of experimentation.

Orthogonal experimental designs are arrangements of the independent variables such that for all pairs j, k, the sum over the data sets $i = 1, 2, 3, \dots, n$ vanishes, i.e., $\sum_i x_{ij} - x_{ik} = 0$, for $j \neq k$. In the following discussion the term dimension will refer to the number of geometric coordinates required to present the response itself. The term order of the model will refer to degree of the polynomial forming the model (first degree = first order, second degree=second order etc.). The order of the design is related to the order of the model; that is, a first order design can be used with linear first order models of one, two,

three more dimensions but not with the second order models. While second order design can be used for order models, more experimentation would have to be carried out with such designs than is actually needed.

A factor denotes any of the experimental variables which are deliberately varied in the experiments, such as mill speed, ball load, ball size, etc. A factorial experiments is one in which all possible combinations of the factors are used. For example, if two variables are to be controlled at two levels each, then there are four possible combinations of experimental conditions; the experiment is termed as a two level factorial experiment, often abbreviated 2^2 designs.

In the 2^2 factorial designs, each value can be portrayed geometrically as the corners of a square in two dimensions (see Fig. 2.8). If x_1 represents percent critical speed and x_2 represents the ball size, five experiments had to be carried out at pairs of (speed, ball size) values such that when properly transformed the factorial design is obtained.

A very simple orthogonal two-level factorial experimental design (2^2 designs) was carried out for a first-order two dimensional model. Several models were considered and one that best suited the experimental data is shown below:

$$y = \beta_0 + \beta_1 x_1 + \beta_2 x_2 + \beta_3 x_1^2 + \beta_4 x_2^2 + \varepsilon \quad (1)$$

The coefficients i.e. β_0 , β_1 , β_2 , β_3 , β_4 were calculated using Sigma-plot software for two different responses (degree of flattening and water coverage). The final model equations obtained are given below in Eqn. (2) and (3).

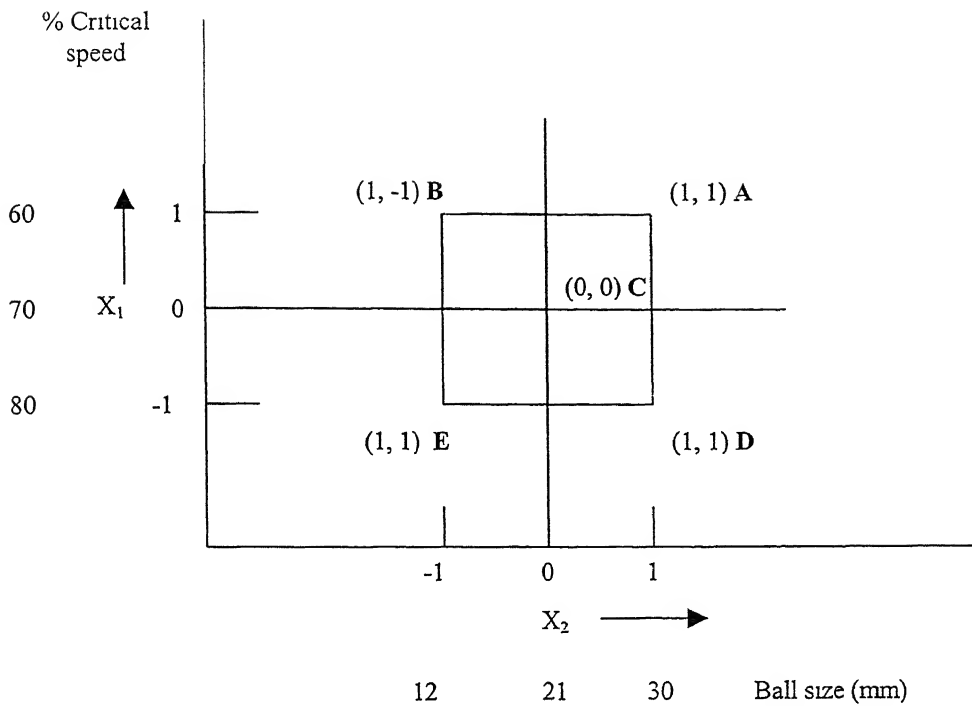


Figure 2.9 Two-level factorial designs for the factors Percentage of critical speed and ball size.

$$y_1 = 2.742 - 0.033 \times x_1 - 0.0065 \times x_2 + 2.428 \times 10^{-4} \times x_1^2 + 8.971 \times 10^{-6} \times x_2^2 \quad (2)$$

$$y_2 = -1.8 \times 10^{-4} + 500.3 \times x_1 + 28.92 \times x_2 - 3.431 \times x_1^2 - 0.07738 \times x_2^2 \quad (3)$$

In the above equations y_1 , and y_2 are degree of flattening and water coverage respectively, and similarly x_1 , and x_2 are the percent critical speed and ball size. After knowing the coefficients, calculated responses were found out. Calculated response and percentage of error are given in the Table 2.4 and 2.5. In case of 70 %, the critical speed and with average diameter 21mm (mill running with first 8hours with existing ball and next 8hours 12mm ball) gives minimum error.

Table 2.4 Calculated response and percentage of error for degree of flattening.

Variable x_1 %Critical speed	Variable x_2 Ball size(mm)	Measured Response (Degree of Flattening)	Calculated Response	% of Error
60	30	1.19	1.1801	0.99
60	12	1.28	1.2901	0.78
80	30	1.19	1.2002	1.02
80	12	1.32	1.3102	0.98
70	21	1.22	1.2201	0.01

Table 2.5 Calculated response and percentage of error for water coverage.

Variable x_1 %Critical speed	Variable x_2 Ball size(mm)	Measured Response Water Coverage (cm ² /gm)	Calculated Response	% of Error
60	30	471	466.1580	1.02
60	12	0	3.0173	0
80	30	785	783.5554	0.18
80	12	408.2	402.2173	1.46
70	21	863.5	865.3580	0.21

2.3.1 Surface Response

The model response for the water coverage and degree of flattening is shown in Fig. 2.10 as surface plots. It is seen that at 80 % critical speed and with a 12 mm ball charge the degree of flattening is maximum. On the other hand the water coverage is maximum for 70% critical speed and 30mm ball charge. Put together it appears that 70% critical speed and 21mm ball load appears to be the best compromise between optimal degree of flattening and water coverage

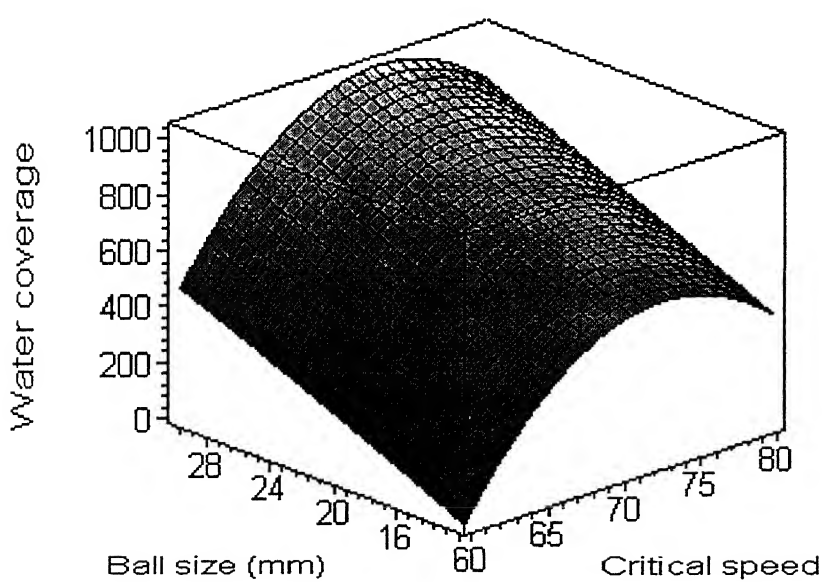
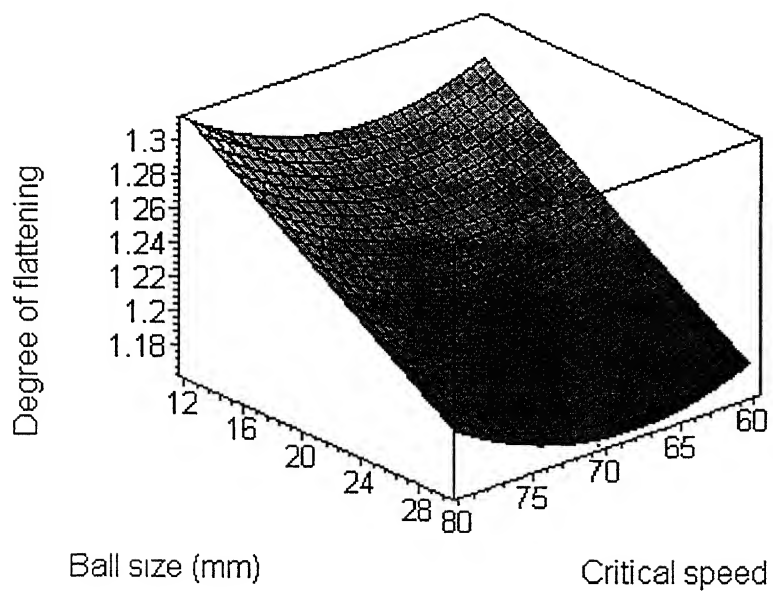


Figure 2.10 Surface plots for two measured responses: top—degree of flattening; below—water coverage.

2.3.2 Effect of mill speed and ball size

The mill speed is a key parameter that controls the grinding environment inside the mill. Typically ball mills operate between 60 to 80 % of critical speed. The critical speed of the mill is defined as the rotational speed at which the balls just start to centrifuge. The power draft of the mill increases with increase in mill speed. The breakage rate of particles also increases with mill speed. The tumbling action and the rates of breakage depend how much of the mill volume is filled with ball. For a given ball load the mill speed must be correctly set that provides sufficient cataracting action to flatten the coarse particle and at the same time provides enough cascading action for fine grinding. If the balance of the charge action between cataracting and cascading charge is not right then particles either over or under grind.

An important general principle is that to avoid the production of excess fines in a continuous milling operation, it is required to remove material which is already fine enough from the mill as fast as possible thus avoiding over grinding. This is done by close-circuit operation of the ball mill.

Figure 2.11 shows the effect of mill speed on grinding of metal powders. The curves corresponding to A and D show the effect of speed on the variation of weight mean diameter at 60 and 80 % of critical speed respectively. Clearly at 80 % critical speed particles are ground to a much larger extent compared to 60 % critical speed. Finer distribution gives rise to increase in water coverage up to 70% critical speed (see Fig. 2.10). Further increase in speed although makes the size distribution even more finer as evident from Fig 2.11 and Fig. 2.12, it is the presence of excessive amount of fine that is believed to be responsible for the drop in water coverage. The fine particles tend to agglomerate and thus do not expose the entire surface area to the water thus the water coverage decrease. In a practical sense it is therefore imperative that the excessive grinding leading to generation of excessive amount of fines be avoided. This can be done by properly monitoring the performance of air cyclone and the air draft through the mill.

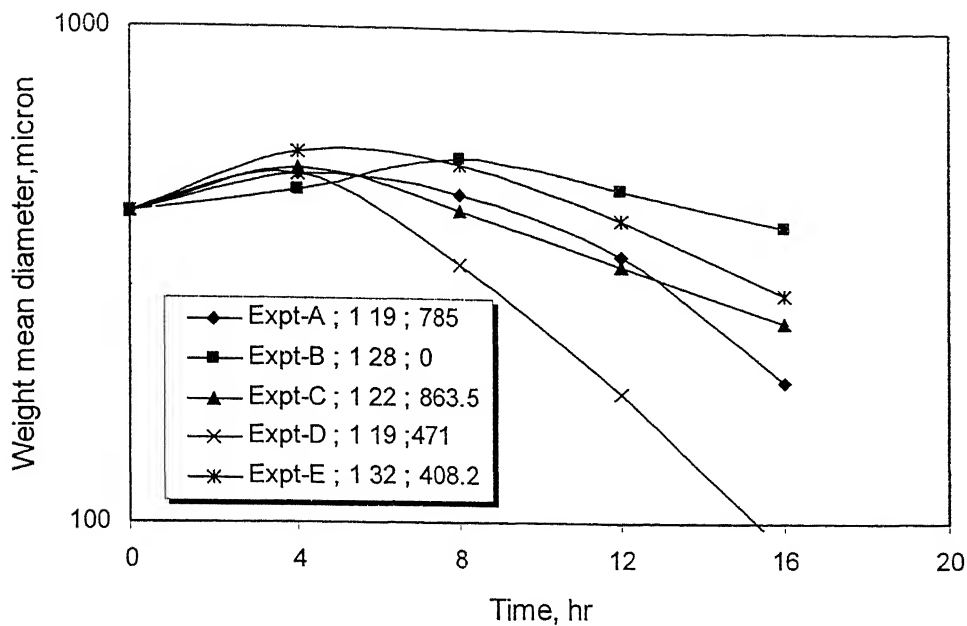


Figure 2.11 Variation in weight mean diameter with time; Experimental conditions at A, B, C, D, and E are defined in Fig. 2.10.

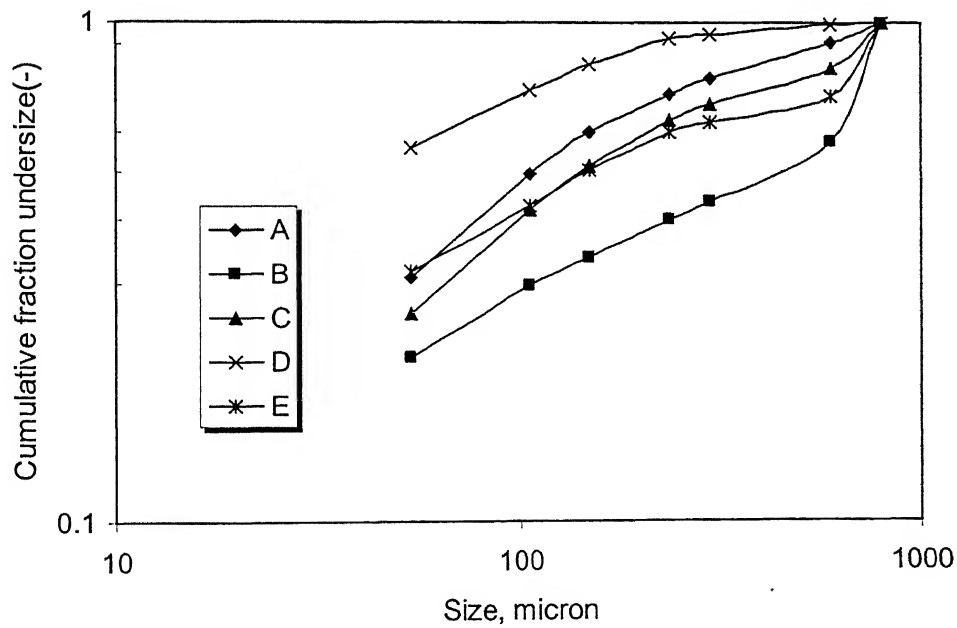


Figure 2.12 Size distribution after 16 hours of grinding; Experimental conditions at A,B,C,D, and E are defined in Fig. 2.10.

The rate of ball to ball contact per unit time increases as ball diameter decreases as the number of balls per unit volume of the mill increases as $1/d^3$. Thus the rates of breakage of particles of a given size are higher for smaller ball diameter. It also appears that the greater impact force of a collision involving a larger ball produces a somewhat bigger portion of fines for a given particle size. Thus the lower specific rate of breakage due to larger balls is partially compensated by the production of a larger portion of fine fragments. Nevertheless, the breakage is minimized and flattening is increased with the use of smaller size ball as evident from Fig 2.10.

In Fig. 2.11 the effect of ball size is clearly evident. The curves A and B represent grinding data corresponding to 30 mm and 12 mm balls respectively at 60 % critical speed. Similarly curves D and E represent grinding data corresponding to 30 mm and 12 mm balls respectively at 80 % critical speed. The grinding behavior is such that larger balls produce more flaky and fine powder. For best result the ball size must be matched to the operating speed, total ball load and the size of the particles being ground. In general, it is observed that the degree of flattening increases with decrease in ball size for a given mill speed. Smaller balls will slow down the breakage kinetics thereby reducing the throughput of the mill and larger balls will lead to breakage before flattening of the particles. Therefore the size of the ball must be judiciously chosen to strike a compromise between breakage and flattening.

As far as flaky powder production is concerned the particles are required to go through plastic deformation before breakage. As shown in Fig. 12 the size distribution corresponding to Experiment D is the finest but the particles need not be flaky because the corresponding water coverage is low. Thus in a practical situation grinding can be done in stages to achieve optimum water coverage and flattening. A comparatively coarser ball size is required during the earlier stages of grinding. But the question arises as to what should be the correct size. The correct size must be decided by minimizing the breakage or generation of fines in the first stage. Ball size for subsequent stages can be scaled down from the size of the ball employed for first stage.

2.3.3 Water Coverage

Water coverage is an indication of the leafing behavior or flakiness of powders. Water coverage of powder is simply formation of a continuous film of metal on water through surface tension. The higher the surface tension, the more rapid and complete is the leafing. It is interesting to note that the leafing property do not increase with the fineness of powder. Fig. 2.13 shows the variation in water coverage with the amount of -45 micron particles. Clearly, the powder sample that had more than -45 micron resulted in lowest water coverage. It should be noted that the powder samples were collected after 16 hrs grinding under varying conditions. Thus for maximization of the leafing property it is essential to have the correct distribution of particles. In this context the size distribution analysis of the three powder samples is quite crucial.

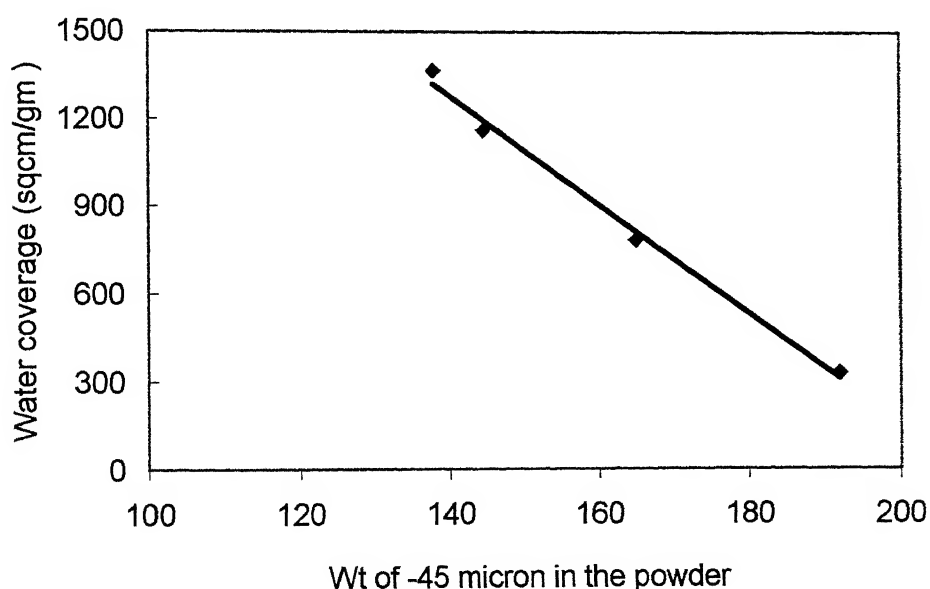


Figure 2.13 Variation in the water coverage with the amount of fines (-45 micron)

2.4 Particle Characterization

The powder sample obtained under the optimal conditions of grinding was characterized to compare with industrial grade samples. Three samples were collected from three different sources and designated as A, B, and C. All the samples were first viewed under electron microscopy to identify morphological features and then their size distributions were measured by using laser particle size analyzer.

2.4.1 Scanning Electron Microscopy

The particulate material samples obtained from the three different sources were prepared for the SEM analysis. Here the particles were washed with hexane to remove the stearic acid film. The aggregate samples were viewed at magnification of 500X and the single particles were viewed at 5000X. Figs. 2.14 to 2.16 show the SEM photographs of A, B, and C samples respectively. SEM photographs of laboratory ground particles are also shown in Fig. 2.17. These photographs bring a good comparison between the individual particle samples and the main differences are outlined below.

- The photographs of the aggregates clearly show that the C powder is largely equiaxed. The A and B particles are of irregular shape; should be considered more elongated than equiaxed. The shape of the particles has got more to do with the quality of the atomized powder than the grinding process.
- Generally more the irregular shape, the finer is the powder and the worse is the flow of the powder in specific applications. Therefore the flowability of C particles is expected to be the best.
- The A and B powders show considerable amount of ultrafine particles. In other words, one would expect a wider size distribution of these particles compared to the C powder sample.

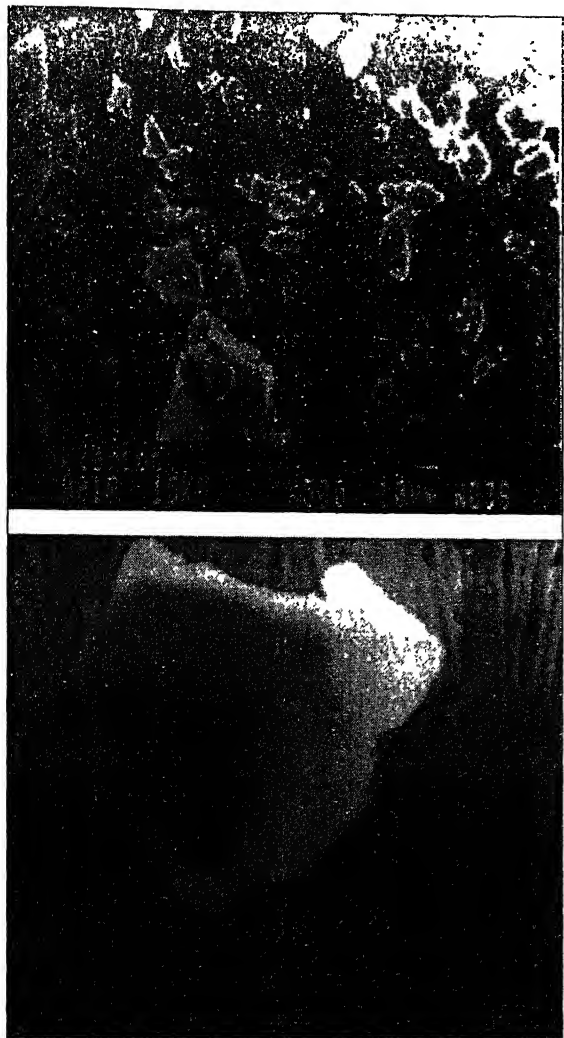


Figure 2.14 Typical SEM images of the Orion powder sample
(a) aggregate at 500X
(b) Single particle at 5000X

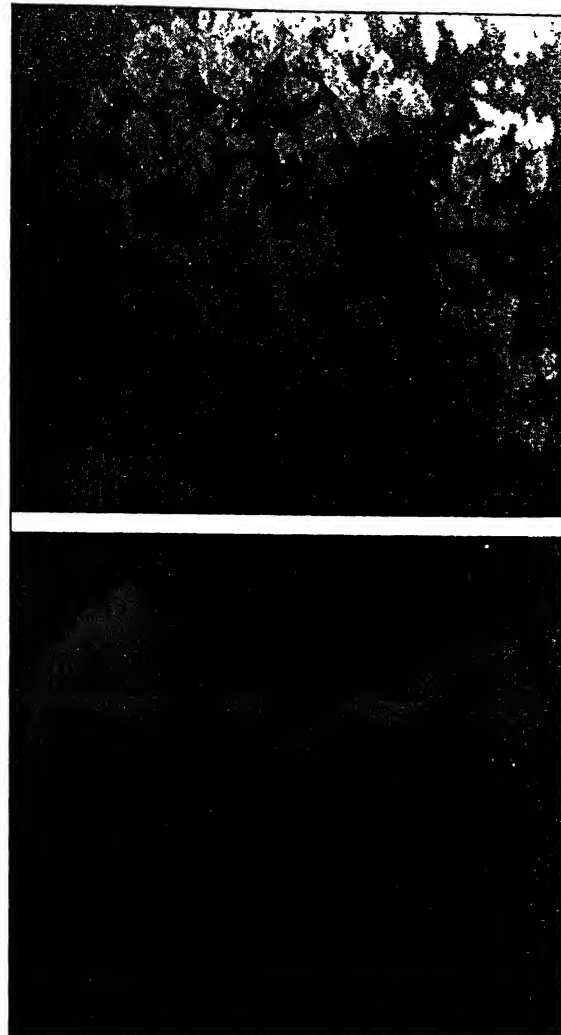


Figure 2.15 Typical SEM images of the Mepco powder sample
(a) aggregate at 500X
(b) single particle at 5000X



Figure 2.16 Typical SEM images of the English powder sample
(a) aggregate at 500X
(b) Single particle at 5000X.

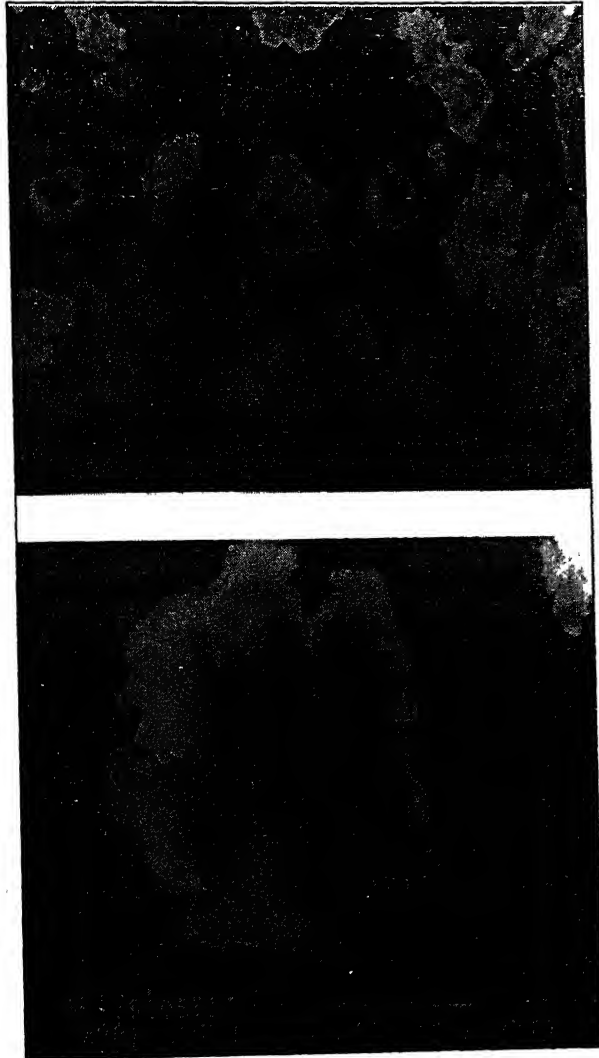


Figure 2.17 Typical SEM images of the Stearic acid powder sample (a) aggregate at 500X (b) Single particle at 5000X.

2.4.2 Size Distribution

In general, powders are designated in terms of a simple size range. Historically these are often quoted in terms of the mesh size used in traditional sieving classification. While sieves may still be used for classification of powders, measurement of size is frequently carried out by instruments using laser light scattering. These plot the size of the powder particles in terms of an "equivalent" diameter of a projected sphere. For spherical powder this is quite accurate, but for irregular shapes (i.e. most material) the sizes given will always be larger than the "actual" sizes. The plot is usually drawn in terms of percentage finer than a stated size.

In many applications, any significant shift in size distribution will have important consequences. Powders finer than usual will tend to oxidize while coarser material may not be suitable for the desired application. As a result, more and more end users are paying particular attention to the distribution of powder on a lot by lot basis.

Fig. 2.18 shows the size distribution of the three different samples. As expected along the lines of microscopic analysis explained earlier, the C powder sample is narrowly dispersed compared to the other two samples; 90 % of the particles are in the size range of 2 to 12 micron. The B powder sample conforms to the same size range but the distribution is slightly different. In contrast, the A powder sample shows excessive amount of fines. No particle is found to be coarser than 5 micron. This suggests that excessive amount of grinding leading to particle breakage is occurring. The size distribution appears to be the main drawback of the A powder sample. It is believed that the presence of ultra fine particles not only reduces the water coverage but also reduce the luster by an enhanced surface oxidation. It has been determined that the water coverage decreases beyond a certain fineness in grinding. More over the fines are susceptible to fast oxidation.

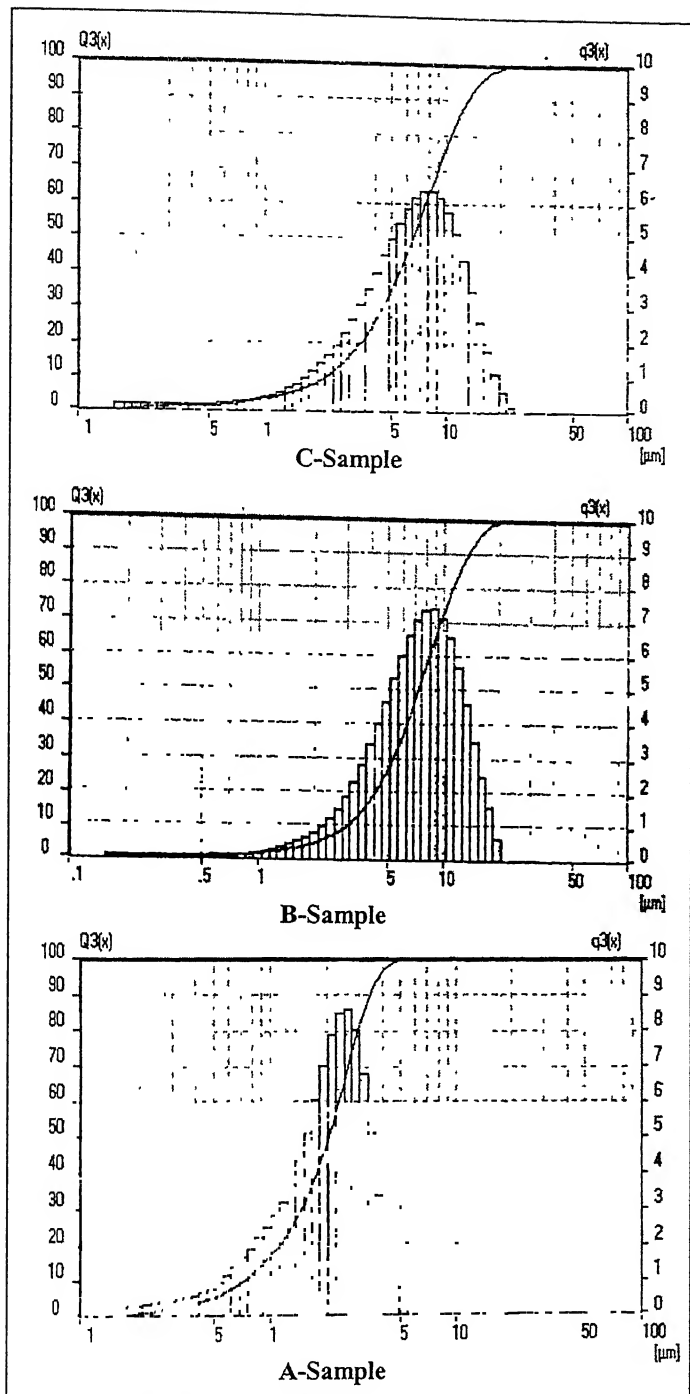


Figure 2.18 Particle size distribution of as received powder sample obtained from the three different sources: Orion, Mepco and English.

Figure 2.19 shows the size distribution of the laboratory prepared sample. The sample ground with stearic acid shows 90 % of the particles in the size range of 6 to 40 micron. In comparison to powder sample C, only 80% of particles are in the size range between 2 to 12 micron. Then again these particles are prepared in batch manner. Further grinding for longer period of time would generate identical powder sample corresponding to C.

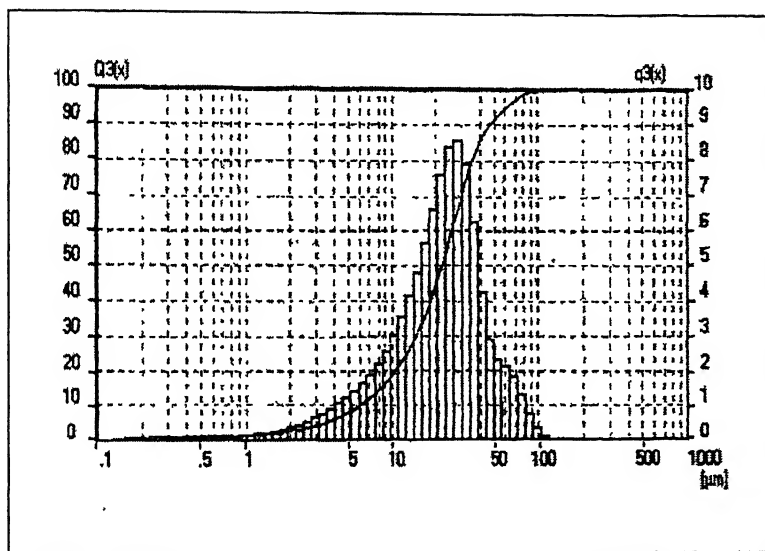


Figure 2.19 Particle size distribution of powder sample after 16 hours of grinding.

CHAPTER 3

ANALYSIS OF INDUSTRIAL DATA USING MILLSOFT

M/s Orion Metal Powder Pvt. Ltd located at Ranikhet, Uttaranchal is involved in non-ferrous powder manufacturing business for several years. The original set-up was commissioned in 1982 and after take over by M/s Orion Metal Powder Pvt. Ltd., the plant is running uninterrupted since 1990. It has a total production capacity of 720 M.T. per year

The processing of the metal powder is done in stages starting with melting through atomization, annealing, grinding, and polishing. Ball mills are involved in the grinding operation that are known to be energy intensive and therefore much more attention was required to optimize the running of these mills to minimize power consumption and maximize productivity at the highest quality. While very little control can be exercised in the plant due to lack of sensors, the capacity of the grinding circuit could only be increased by constant monitoring of the process relying on operating experience.

A plant trip to Ranikhet was made to collect data on the grinding circuit. Basically the particles were broken to the powder form in several stages of grinding. The first stage of grinding is done in open circuit and the second stage grinding is done in close circuit. As a first step towards process optimization the first stage grinding circuit was simulated using the software called Millsoft. The software uses the discrete element method to track the motion of balls inside the grinding mill. To track the position of balls/rock, the interactions between individual entities are modeled through a spring-dashpot representation. As a dynamic process, the evolution of contact forces gives rise to incremental displacements of the particles by applying Newton's second law of motion. Details of this software can be found elsewhere [16].

The results of first stage simulation brings into focus the inefficient operational practice then must be improved. The mill was simulated for the plant data as shown in Table 3.1. Figure 3.1 shows four different snapshots at different interval of time. It is quite clear that the balls are more or less centrifuging inside the mill. At certain times the charge is raining from the top. Under these conditions grinding is definitely highly inefficient.

Table 3.1 Typical plant practice data

Ball load	1000 kg
Particle weight	100 kg
Rpm	42
Mill diameter	0.8m
Number of lifters	6
Lifter width	2.5 cm
Lifter height	2.5 cm
Motor rating	15 KW

The processing capability of a mill is greatly affected by design and operating variables of the mill. The key issue here is the field of breakage. The motion of charge inside the mill can be viewed as a field of breakage generated as a result of the internal profile of the lifters and the rotational speed of the mill shell. The particles entering through the feed port is ground by this field and, if it is sufficiently ground, the particles leave the mill. The field of breakage influences the hold-up mass in the mill. More over, the particles that are ground when reach the free surface of the charge tend to get swayed by the air and exit the mill. Thus the pressure differential is the key operating parameter that must be constantly monitored and controlled.

The particle quality, field of breakage and flow through the mill influence each other and the net effect is the build-up of a hold-up level in the mill, which draws a certain power and this power draft is clearly linked with mill throughput. If the interaction can be understood then mill capacity can be understood much more clearly.

Then the expectation of increasing capacity at the same level of power draft by one means or another can be safely evaluated.

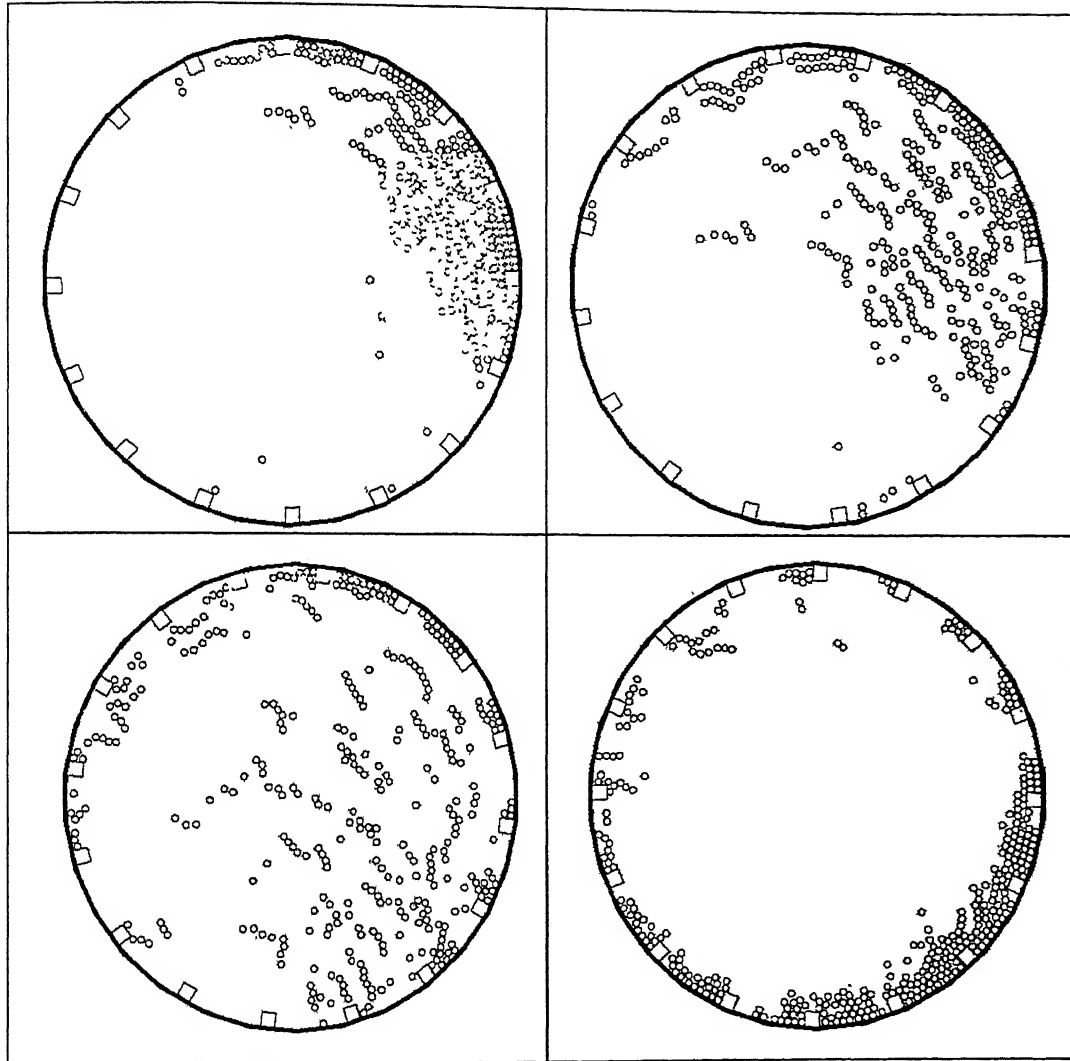


Figure 3.1 Charge motion inside the tumbling mill (first stage grinding) at 42 rpm.

The efficiency of the mill depends on the breakage rate of particle present in the mill. The breakage rate in turn depends on the power draft of the mill for the simple reason *work done (in fracturing ore particles) is directly proportional to energy input*. The power delivered to the mill should be efficiently transferred to the bed of ore

particles in the mill to achieve maximum efficiency. There are four principal operational factors that influence this power delivery. They are: *Mill filling*, *Mill rotational speed*, *Design of Shell lifters*, and *pressure drop across the mill*. Some of these parameters are tackled through simulation using Millsoft.

In order to optimize the capacity of the mill a simulation campaign was undertaken using Millsoft[®]. Here the mill was assumed to be driven by a 15 KW motor. The simulation was carried out with the mill parameter as obtained from the plant (see Table 3.1).

Two types of lifter profiles were considered for the simulation purpose: existing lifter profile and a modified lifter profiles. These two lifter profiles are shown in Fig. 3.2. As evident from the figure the square cross section lifter corresponds to the existing profile of the plant. It is clear that this type of lifter is going to result in excessive throw. The height of the lifter is more than twice the diameter of the balls. Therefore it is going to hold lot of balls and throw them to the other side of the mill. At the point where the balls are going to hit the mill shell, there is very little chance that they are going to catch particles. This scenario is going to lead to wastage of energy through unnecessary impacts.

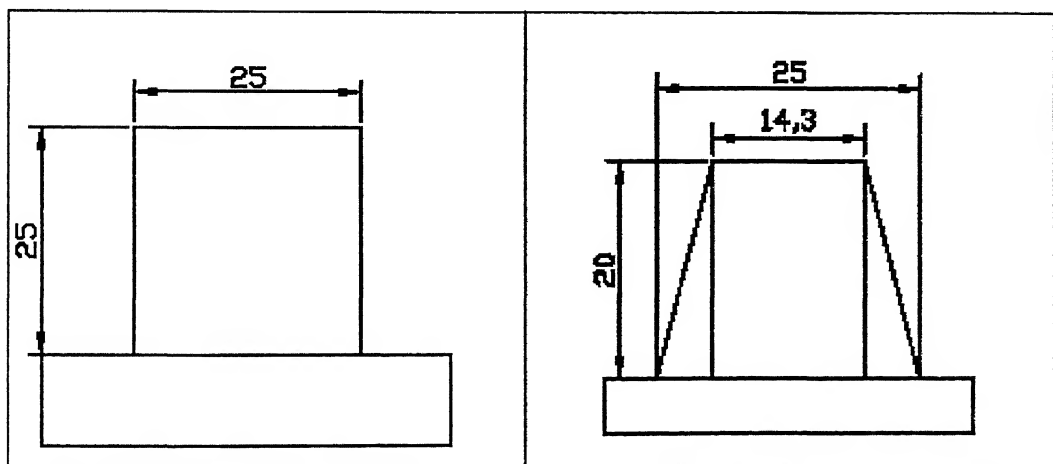


Figure 3.2 Lifter profiles used in the simulations (All dimensions are in mm).

To understand how the charge is moving inside the mill, Millsoft was used to simulate the 0.8-m diameter mill at 26 and 32 rpm. The profile of the ball charge at various intervals of time is shown in Fig. 3.3 and 3.4. Following points emerge from the analysis of the snapshots:

- First of all the mill seems to be running far below the rated capacity.
- The motor is used below its peak power delivering level: it draws 7 and 9 KW at 26 and 32 rpm respectively.
- The particles are loose while in flight and impact at various locations on the mill shell between 7 to 9 O'clock positions. The trajectories are not uniform because the gap between lifters is too large.
- Overall charge profile is definitely not the most desired one. With about 10% ball load the dynamic pressure of the charge is very less. Thus the breakage rate of particles is believed to be less. This alone undermines the achievable capacity of the mill.
- The mill speed could be decreased from 32 rpm to avoid unnecessary impact but then again the cataracting trajectories would be lost. This will again reduce the breakage rate. For effective grinding both cataracting and cascading profiles of the charge are essential.

It is felt that the situation could be improved by increasing the number of lifters and decreasing the speed to optimize the capacity.

Lifters are not only consumables for protection against wear, but also critical machine elements. They transfer power to the mill charge and govern the pattern of energy distribution inside the mill, including affecting the grinding kinetics. A good design must take these aspects into consideration and optimize the performance of lifters for the full duration of their useful life. Assuming that the mill can only draw up to 15 KW the mill performance is optimized by increasing the number and changing the shape

of lifters, and increasing the mill filling. At the end, the speed is controlled to obtain the peak power and correct charge profile.

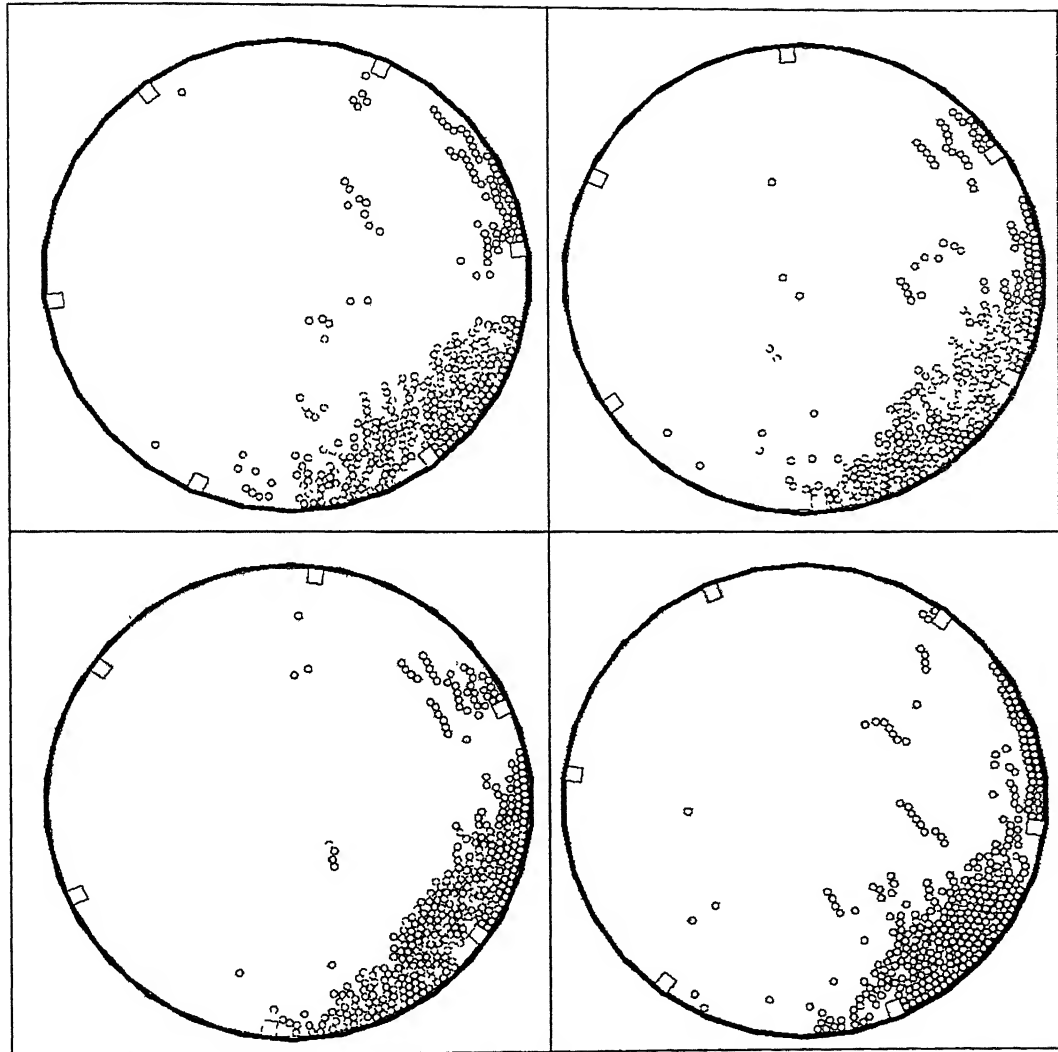


Figure 3.3. Snapshots of charge motion inside the mill (Mill diameter = 0.8 m; ball load = 10%; ball diameter = 12 mm; mill speed = 26 rpm; power draft = 7 KW).

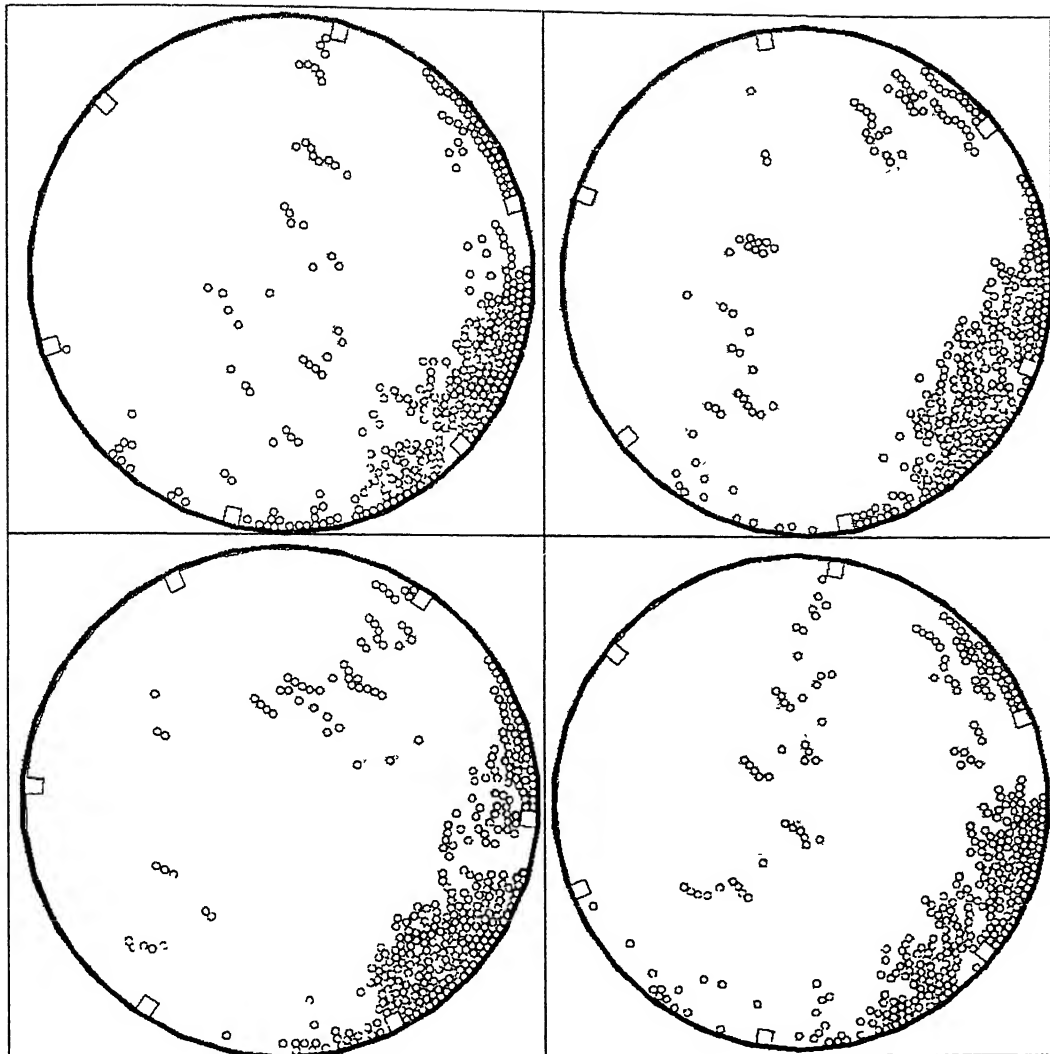


Figure3.4. Snapshots of charge motion inside the mill (Mill diameter = 0.8 m; ball load = 10%; ball diameter =12 mm; mill speed = 32 rpm; power draft = 9KW).

The simulation result shown in Fig.3.3 and 3.4 clearly demonstrates that the existing milling practice is not highly desirable. Improvements can be made by simply increasing the number of lifters and the ball load. Figure 3.5 shows the results of simulation where the number of lifters were increased from 6 to 12 and finally to 24. Also the ball load was doubled (20% mill filling). It is observed that by increasing the ball load at 26 rpm the power draft of the mill increases from 7 to 11 KW. This can be seen from Fig. 3.5 (a). By increasing the number of lifters from 6 to 24 the power draft increases up to 13 KW. This improvement is possible due to the action of the lifters that holds the charge in position. However, the charge motion is not adequate for breaking the metallic powder.

For the breakage of atomized powder in the size range of 400-500 micron, two distinct charge profiles are needed. The cataracting charge is required for flattening of the particles and the cascading charge is required for breaking the particle. The cataracting charge must capture particles. Therefore the cataracting balls must hit the toe of the charge between 6 and 7 O'clock position. At the same time the ball size must match with the particle size being ground. At 26 rpm, the charge profile didn't show much cataracting action. Therefore one could increase the mill speed. But at higher speeds the rectangular lifters are known to throw the charge beyond the toe region. And for this reason inclined lifters are used that allows operation at a higher speed while maintaining the right proportion of cataracting and cascading charge.

To improve the charge profile a trapezoidal set of lifters is used. The lifter dimensions are shown in Fig. 3.2. Here, the simulation was done with identical condition as before i.e. 26 rpm, 20% filling, 24 lifters, and 12 mm ball but the shape of the lifter was changed from rectangular to trapezoidal. The power draft reduced from 13 to 11 KW (compare Fig 3.5 (c) with Fig. 3.6 (a)) and the charge profile didn't show much cataracting action. By increasing the speed from 26 to 36 rpm the desired charge profile was attained (see Fig 3.6). It is believed that for best result the mill must be operated between 30 and 36 rpm to get the peak power and best grinding results.

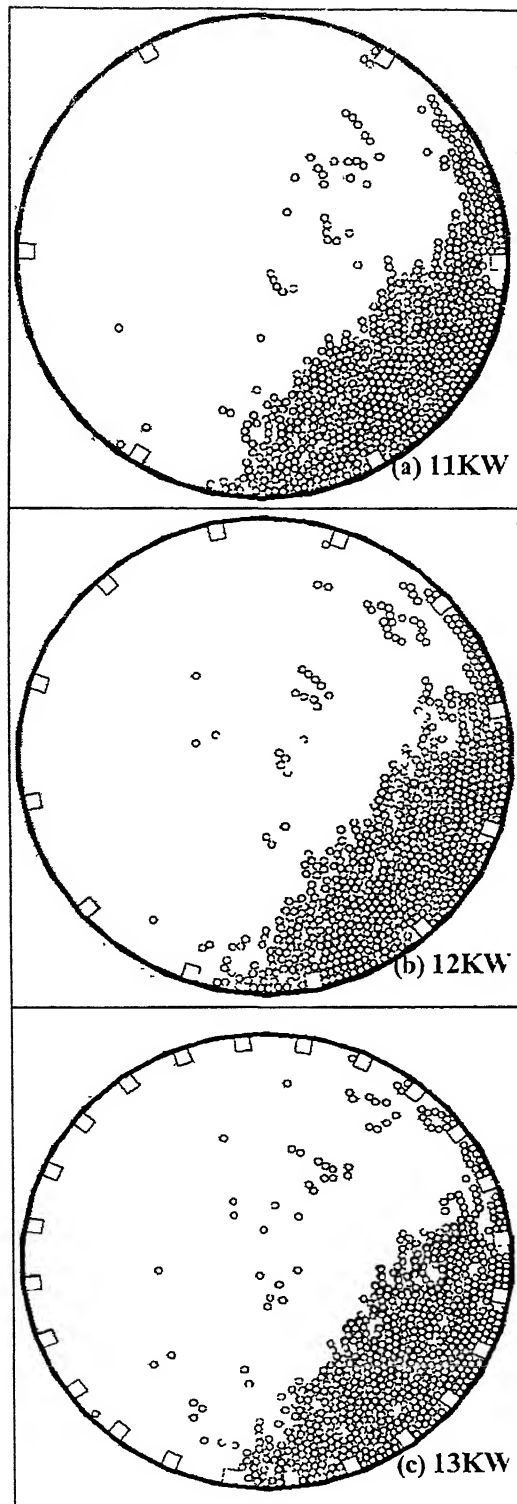


Figure 3.5 Snapshots of charge motion inside the mill: effect of lifter configuration
(mill diameter = 0.8 m; ball load = 20%; ball diameter = 12 mm; mill speed = 26 rpm).

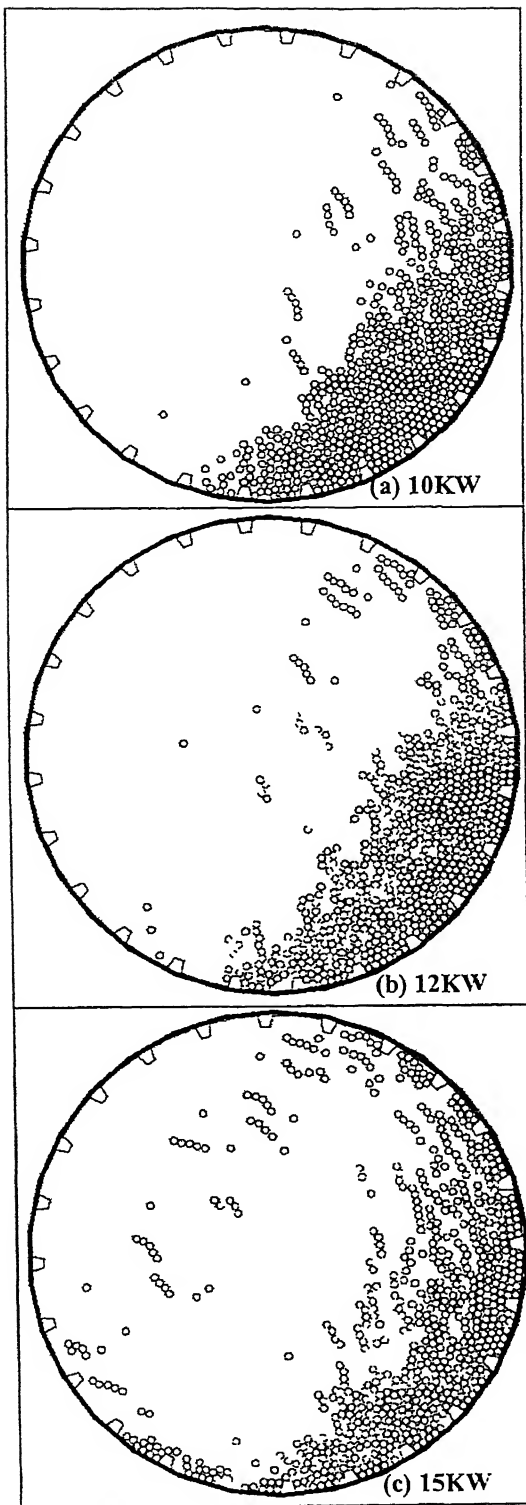


Figure3.6. Snapshots of charge motion inside the mill: effect of lifter shape; (mill diameter = 0.8 m; ball load = 20%; ball diameter =12 mm; mill speed: (a) 26 rpm (b) 30 rpm (c) 36 rpm)

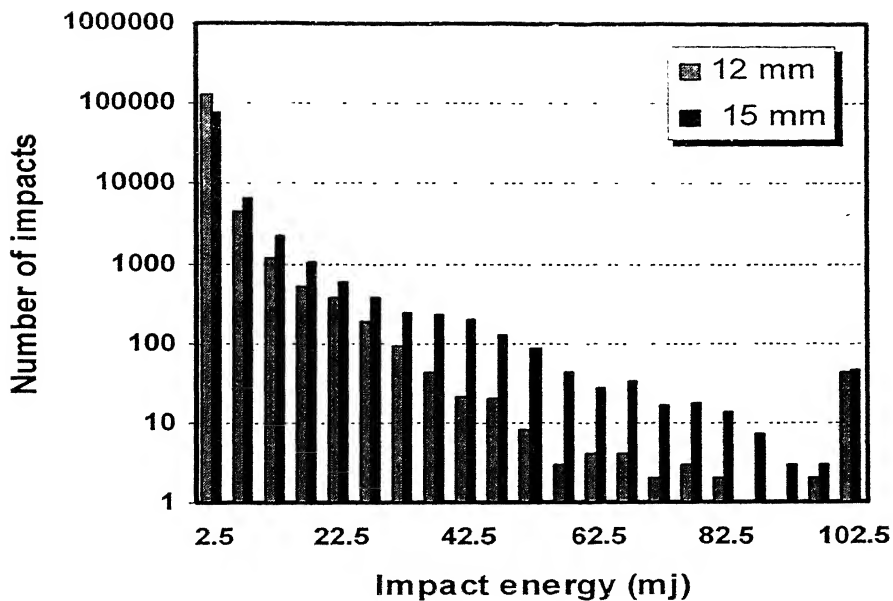


Figure 3.7 Impact energy spectra for two different mill simulations where only the ball size was changed.

The ball size is a key parameter that must be carefully set. In the laboratory experiment better results were obtained by using 20 mm balls. To decide the correct ball size the mill simulation corresponding to Fig 3.6 (c) was repeated. Keeping all parameters same, only the ball size was increased to 15 mm. As expected, since ball load and mill speed were same, both simulations yielded comparable power draw. At this stage, one would like to know how the energy gets distributed amongst all possible collisions recorded during the simulation period. All the collisions and their corresponding impact energies were sorted. The data are presented in Fig. 3.7 that shows the impact energy spectra corresponding to the two cases.

Careful analysis of Fig. 3.7 reveals that the number of impacts in the lower impact energy range up to 25 mJ is comparable in each case. At the same time the high energy impact greater than 100 mJ are also comparable. The number of impacts in the middle range of energy makes all the difference. As evident from the figure that the number of impacts in the middle ranges (25 – 100 mJ) is significantly higher when 15 mm balls are used.

In a 0.8-m diameter mill when a 12 mm diameter ball falls from the maximum height, a total of 50 mJ is transferred to the particle and it is double that amount for a 15 mm ball. Therefore, as far as cataracting profile is concerned either 12 or 15 mm ball is adequate. But for breakage that takes place in the shear mode within the cascading regime, the 15 mm ball charge will be more effective. Therefore, in the first stage of grinding it is believed that by increasing the ball size to 15 mm the capacity of the mill could be increased.

CHAPTER 4

CONCLUSIONS

In this research work, different experiments were carried out, to find out the optimum conditions of a grinding process involving 70-30 brass particles. Experiments were performed to determine correct operating parameters i.e. material to ball ratio, type of additives, and percentage of additives and ball load. These parameters were determined by considering the degree of flattening, water coverage and luster. Degree of flattening represents the amount of plasticity imparted to particles prior to fracture. Water coverage represents the leafing property of the particles. When particles have very high diameter to thickness ratio, the surface properties assume importance compared to the bulk properties. Under these conditions particles tend to form a film on water without wetting.

While determining the optimal parameters a total ball load of 30% has been assumed a priori. It has been determined then that a material to ball ratio of 0.06 gives the best grinding result. Of the three additives tested, stearic acid has been found to give the best result when used in the range of 10 to 20 percent of the material weight. However a detrimental effect of stearic acid on brass through formation of zinc stearate could not be investigated.

Certain other parameters assume importance from a practical point of view. While all the parameters discussed earlier could be adjusted during operation, certain other parameters such as mill speed and constitution of ball load could not be varied. To determine the effect of these parameters, a 2^2 factorial design model has been designed for determining the optimum mill speed and ball size. The response variables were considered to be of flattening and water coverage. It is determined that while determining the optimal speed and ball size a compromise has to be sought between the degree of flattening and water coverage. Higher speed gives rise to finer size distribution

that shows maximum water coverage and highest degree of flattening at about 70% and 80% critical speed respectively for any ball size. At the same time the size of the ball has opposing effect on water coverage and degree of flattening for any given speed. Considering these interactions, for the atomized particles under test (3mm), it is determined that the best grinding conditions correspond to 20 mm ball and 70% critical speed.

The laboratory grinding studies provides a wealth of information that serves as a guideline for improvement in industrial grinding practice. In other words, the laboratory tests point to several areas of improvement as far as grinding is concerned. First and foremost among them is the use of larger size balls during the first stage of grinding. Second, for better water coverage it is not necessary to grind the particles to the finest size range. The optimal grinding can be attained by changing the grinding practice from an impact mode to shear mode. Third, the stearic acid addition and particle to ball ratio is most effective (when set at 0.1% of particle weight and 0.065 % of the ball weight) among all the additives used. Some of the salient features of the present work that may help to improve the actual plant practice are as follows.

1. Leafing properties, shinning and flakiness are higher in case of 0.06 materials to ball ratio. So the optimum condition for material to ball ratio should be maintained at 0.06.
2. Stearic acid is the best additives as compared to paraffin wax and oxalic acid. Shinning and Leafing property/water coverage is higher in case of stearic acid containing 0.1% wt of the material taken for grinding.
3. From the model, it has been found that 70% critical speed with 21-mm ball size gives the best result.

The characterization studies using scanning electron microscopy and size analysis reveal that the particles ground in a batch mode is comparable in terms of size and morphology to that of industrial samples. The shape of the particles after breakage is a matter of concern as one would like to have as much equiaxed particles possible after

grinding. It has been determined that the use of stearic acid as a grinding additive gives uniform size distribution and equiaxed shape.

While particle shape isn't always a variable that can be controlled, some size-reduction methods may be beneficial if shape is important. Typically, when shear is the primary mechanism for reduction, some control of shape may be attained. When compression and impact are at work, particles tend to fracture in a more-random manner. Therefore, for equiaxed particle formation the grinding period can be increased to attain the same degree of fineness. This can be done by controlling the dynamic profile of the charge through proper lifter, mill speed and ball loading.

M/s Orion Metal Powder, are in the business of brass powder making for the paint and lacquer industry. The grinding at their works is done in stages. The first stage of grinding is done in a 0.8-m diameter mill. The mill is fitted with six lifters; it uses 12 mm balls for a ball load of 10% of mill volume; the mill speed is set at 42 rpm. This mill is driven by a 15 KW AC motor. As part of this thesis work the mill operation is simulated to determine operational bottlenecks and suggest remedial measures.

Several simulation tests were carried out using Millsoft which is proven software for tumbling mill analysis. It was determined that the current practice is highly inefficient both in terms of energy and grinding efficiency. At a 10% fill level and 42 rpm, most of the charge is trapped between the lifters and cataracts. It is also observed that as the mill is filled to 20%, progressively the cascading free surface rises higher and becomes more angular in shape. The amount of cataracting material is essentially independent of the fill level for a given set of lifters since the same amount of material is trapped between the lifters for all fill levels. By increasing the number of lifters from 6 to 24, increasing the ball load to 20%, and decreasing the mill speed to 32 rpm it has been demonstrated that the mill draws peak power. Under these operating conditions the mill is expected to double its capacity and utilize power in an optimal manner.

APPENDIX A

A.1 Material to Ball ratio

These grinding experiments were carried out in a 35cm diameter and 17.5 cm height cast iron made ball mill. Mill filling is taken as 30% by mill inner volume. Mill is placed over a rubber roller and rotated with electric motor. Mill critical speed was taken at 70% critical speed. Monosize particles of (-32, +50) mesh are used in these experiments.

In this experiment, mill speed is maintained at 70% critical speed. Monosize brass sample of range (-30, +50 mesh) is taken. Weight of the material taken is 2.5 Kg and weight of the ball is 25 Kg. Adding stearic acid (additives) 0.1% wt of material in each 4hrs grinding interval. Cumulative mass fraction retained finer for different material to ball ratio were given in the table A.1, A.2 and A.3.

TableA.1 Cumulative undersize finer after 16hrs grinding, material to ball ratio=0.1

Size(μm)	4hrs	8hrs	12hrs	16hrs
800	1	1	1	1
600	0.6269	0.5563	0.8713	0.9958
300	0.1412	0.236	0.5915	0.9475
250	0.1126	0.1797	0.4984	0.9027
150	0.0379	0.0932	0.3137	0.7504
106	0.0176	0.0549	0.2102	0.5965
53	0.0059	0.0217	0.098	0.3072
45	0.002	0.0077	0.0587	0.2624

TableA.2 Cumulative undersize finer after 16hrs grinding, material to ball ratio=0.075

Size(μm)	2hrs	4hrs	8hrs	12hrs	16hrs
800	1	1	1	1	1
600	0.78	0.5774	0.8822	0.9946	0.971
300	0.2533	0.1859	0.612	0.9332	0.9074
250	0.1592	0.1297	0.5181	0.8831	0.8734
150	0.0587	0.0595	0.3304	0.7217	0.8011
106	0.0186	0.0341	0.2227	0.5545	0.6648
53	0.006	0.014	0.1049	0.2839	0.395
45	0.0036	0.0083	0.0024	0.2222	0.3253

TableA.3 Cumulative undersize finer after 16hrs grinding, material to ball ratio=0.06

Size(μm)	1hrs	2hrs	4hrs	8hrs	12hrs	16hrs
800	1	1	1	1	1	1
600	0.8659	0.6854	0.5078	0.9565	0.9581	0.9717
300	0.275	0.1863	0.196	0.8016	0.8911	0.912
250	0.1614	0.1123	0.1339	0.7261	0.8561	0.8791
150	0.0304	0.0354	0.0681	0.5241	0.7668	0.8207
106	0.0107	0.0163	0.0399	0.3752	0.5828	0.7003
53	0.003	0.0056	0.0134	0.1812	0.2334	0.2275
45	0.0023	0.004	0.0053	0.1398	0.1431	0.1043

A.2 Different additives used

Experiment is carried out in the same mill (Diameter=35cm, Height=17.5 cm). Mill filling is taken as approximately 30% by inner mill volume. In these experiments material to ball ratio is maintained at 0.067(Wt of material=1.32Kg, Wt of ball=19Kg). Critical speed of mill was taken at 70% critical speed. Adding stearic acid, oxalic acid and paraffin wax 0.1% weight of material after each 4 hours of grinding. Cumulative mass retained for different additives were shown in the table A.4, A.5 and A.6.

Table A.4 Cumulative undersize finer after 16 hrs of grinding with stearic acid

Size(μm)	4 hr	8 hr	12 hr	16 hr
800	1	1	1	1
600	0.4493	0.71872	0.9394	0.9743
300	0.20362	0.4669	0.8081	0.92524
250	0.1507	0.39443	0.7466	0.9019
150	0.08062	0.24916	0.5705	0.8266
106	0.05122	0.17074	0.4177	0.7398
53	0.02712	0.07842	0.1937	0.4899
45	0.0218	0.06518	0.1645	0.4513

TableA.5 Cumulative undersize finer after 16hrs grinding with paraffin wax

Size(μm)	4 hr	8 hr	12 hr	16 hr
800	1	1	1	1
600	0.39294	0.60368	0.9606	0.98732
300	0.17954	0.37378	0.8116	0.93492
250	0.13599	0.31818	0.743	0.90402
150	0.07301	0.21228	0.5588	0.7635
106	0.04487	0.15038	0.4336	0.6264
53	0.02007	0.07438	0.2585	0.4076
45	0.01507	0.0583	0.1621	0.2021

Table A.6 Cumulative undersize finer after 16hrs grinding with oxalic acid

Size(μm)	4 hr	8 hr	12 hr	16 hr
800	1	1	1	1
600	0.74305	0.78813	0.7172	0.8443
300	0.3526	0.4472	0.4755	0.6091
250	0.26429	0.3663	0.407	0.5389
150	0.11409	0.2185	0.2651	0.3924
106	0.05689	0.10438	0.1839	0.2977
53	0.01739	0.04317	0.0916	0.1636
45	0.01305	0.0366	0.0802	0.1462

A.3 Percentage of additive (stearic acid) used:

Experiments were carried out in the same ball mill (Diameter=35cm and Height=17.5 cm). Mill filling is taken as approximately 30% by inner mill volume. In these experiments material to ball ratio is maintained at 0.067(Wt of material=1.32Kg, Wt of ball=19Kg). Mill was moving with 70% critical speed. Cumulative mass fractions retained for different percentage of stearic acid were given in the table A.7, A.8 and A.9.

Table A.7 Cumulative undersize finer after 16hrs grinding with 0.4% stearic acid

Size(μm)	4hr	8hr	12 hr	16hr
800	1	1	1	1
600	0.6201	0.9455	0.9949	0.9984
300	0.3628	0.8568	0.9796	0.9938
250	0.2968	0.804	0.9636	0.9855
150	0.1764	0.6501	0.8964	0.9559
106	0.1127	0.5029	0.7954	0.9056
53	0.0473	0.2456	0.5257	0.6902
45	0.0273	0.1841	0.4715	0.6312

Table A.8 Cumulative undersize finer after 16hrs grinding with 0.3% stearic acid

Size(μm)	4hr	8hr	12 hr	16hr
800	1	1	1	1
600	0.6023	0.9202	0.9884	0.9943
300	0.3095	0.7283	0.9573	0.9814
250	0.2403	0.6653	0.9329	0.9651
150	0.1251	0.4977	0.8657	0.9272
106	0.0739	0.3692	0.7694	0.877
53	0.0279	0.1808	0.5107	0.6992
45	0.0176	0.1225	0.4354	0.6366

Table A.9 Cumulative undersize finer after 16hrs grinding with 0.2% stearic acid

Size(μm)	4 hr	8 hr	12 hr	16 hr
800	1	1	1	1
600	0.4202	0.525	0.9485	0.9962
300	0.1777	0.2736	0.8084	0.9591
250	0.1301	0.2206	0.739	0.9364
150	0.063	0.1314	0.5606	0.8635
106	0.0368	0.0878	0.4178	0.7762
53	0.011	0.0392	0.2062	0.5516
45	0.008	0.0285	0.1606	0.4837

Table A.10 Cumulative undersize finer after 16hrs grinding with 0.1% stearic acid

Size(μm)	4 hr	8 hr	12 hr	16 hr
800	1	1	1	1
600	0.4493	0.71872	0.9394	0.9743
300	0.20362	0.4669	0.8081	0.92524
250	0.1507	0.39443	0.7466	0.9019
150	0.08062	0.24916	0.5705	0.8266
106	0.05122	0.17074	0.4177	0.7398
53	0.02712	0.07842	0.1937	0.4899
45	0.0218	0.06518	0.1645	0.4513

A.4 Variation of critical speed and ball size

Grinding experiments are carried out in ball mill having mill diameter 36.3cm and height 17.5 cm. Mill filling is maintained at 30% by mill inner mill volume. In all these experiments additives used as steric acid. Adding stearic acid 0.1% weight of the material after each 4-hours of grinding interval. In these experiments material to ball ration maintained at 0.0067(Wt of material=1.32Kg, Wt of ball=19Kg). These experiments were carried out with 80%critical speed, 70% critical speed and 60% critical speed and with existing ball, mixed ball and 12 mm ball diameter. Cumulative mass retained for different critical speed and ball size were given in the table A.10,A.11,A.12,A.13 and A.14.

Table A.11 Cumulative undersize finer after 16hrs grinding with 80% c.s and existing ball.

Size(µm)	4hrs	8hrs	12hrs	16hrs
800	1	1	1	1
600	0.4967	0.7698	0.9317	0.9913
300	0.2411	0.5425	0.7927	0.9489
250	0.1832	0.4721	0.7344	0.9247
150	0.0997	0.3206	0.6094	0.8239
106	0.0621	0.2296	0.5037	0.728
53	0.032	0.1063	0.296	0.5621
45	0.0269	0.0997	0.2654	0.5363

Table A.12 Cumulative undersize finer after 16hrs grinding with 60% c.s and existing ball

Size(µm)	4hrs	8hrs	12hrs	16hrs
800	1	1	1	1
600	0.5175	0.5551	0.7119	0.9157
300	0.2335	0.3349	0.5324	0.7733
250	0.1719	0.2785	0.4739	0.7205
150	0.0884	0.1723	0.3355	0.6022
106	0.0538	0.1175	0.2476	0.4979
53	0.0252	0.0564	0.1293	0.3063
45	0.0199	0.0367	0.0986	0.2632

Table A.13 Cumulative undersize finer after 16 hours grinding with 80% c.s and 12mm ball (dia)

Size(μm)	4hrs	8hrs	12hrs	16hrs
800	1	1	1	1
600	0.4096	0.3644	0.5453	0.7134
300	0.1278	0.2431	0.4378	0.6337
250	0.1002	0.2159	0.4036	0.6027
150	0.0646	0.1647	0.3296	0.5057
106	0.0467	0.1302	0.2747	0.4304
53	0.0225	0.0764	0.1838	0.3154
45	0.0202	0.0708	0.1765	0.2871

Table A.14 Cumulative undersize finer after 16hrs grinding with 60% c.s and 12 mm ball
(dia)

Size(μm)	4hrs	8hrs	12hrs	16hrs
800	1	1	1	1
600	0.7326	0.3917	0.4762	0.577
300	0.1399	0.1878	0.3076	0.4374
250	0.0888	0.1582	0.2745	0.4018
150	0.0427	0.1133	0.2205	0.3585
106	0.028	0.0887	0.1874	0.2959
53	0.013	0.0525	0.138	0.2123
45	0.01	0.0449	0.1251	0.1493

Table A.15 Cumulative undersize finer after 16hrs grinding with 70% c.s and mix ball
 (first 8hrs with existing ball and next 8hrs with 12 mm ball)

Size(μm)	4hrs	8hrs	12hrs	16hrs
800	1.0	1.0	1.0	1.0
600	0.4845	0.6045	7284	0.8066
300	0.2091	0.3858	0.5573	0.6869
250	0.1539	0.3228	0.5005	0.6384
150	0.0787	0.2064	0.3625	0.5173
106	0.0481	0.1434	0.2736	0.4217
53	0.0235	0.0707	0.1516	0.2618
45	0.0189	0.0607	0.1186	0.2348

REFERENNCES

1. C.G Goetzel, Treatise on powder Metallurgy, Vol.I, Technology of Metal powders and their products, Inersciennce, New York, 1949, pp. 35-76,259-268.
2. H.S. Amin, Trans.Indian Inst.Met., 6 (1952) 285.
3. A.S Morozov and A.I Raichenko, sov.powder Metall. Met. Ceram. 27 (1988) 520.
4. H.Hashimoto and R.Watanable, Mater. Trans. JIM, 31 (1990) 219.
5. M.K. Sureshan, R.Vedarman and M.Ramanujam, in M.Ramanujam,(ed.), Advances in particulate technology-pro. Int. Symp.Particulate Science and Technology, Madras, India, Dec. 1982, Indian Institute of technology, Madras, pp. 185.
6. M.K. Sureshan, Ph.D. Thesis, Indian Institute of Technology, Madras, India, 1982, pp. 222.
7. M.K. Sureshan, R.Vedaraman, and M.Ramanujam, Particulate sci, Techn., pp. 561.
8. Alan Lawley Atomization The production of metal powders, Monographs in P/M series No.1 pp. 8.
9. P.Ulf Gummesson, "Morden Atomization Techniques" , Powder Metall.,, Vol.15, No. 29, pp. 67, 1972.
10. J.K Beddow, The Production of Metal Powder by Atomization, Heyden Press, Philadelphia, PA, 1978.

11. A.Unal, "Production of Rapidly Solidified Aluminum Alloy Powders by Gas Atomization and Applications" , Powder Metall., Vol. 33, No. 1, pp 53, 1990.
12. R.P Fraser and P. Eisenklem, "Liquid Atomization and the Drop size of Sprays" , Trans. Institution Chem. Engineers, Vol. 34, pp. 20, 1986.
13. J.J. Dunkley, "Producing Metal Powders" , Metals and Materials, Vol. 6, No. 6, pp. 361, 1990.
14. E.Klar and W.M. Safer, "High-Pressure Gas Atomization of Metals" , Powder Metall., for High Performance Application, Editors: J.J. Burke and V. Weiss, Syracuse University Press, Syracuse, NY, pp. 57, 1972.
15. Alan Lawley Atomization The production of metal powders, Monographs in P/M series No.1 pp. 22.